DEFENCE **R&D** DÉFENSE

Global Shoreline Mapping from an Airborne Polarimetric SAR:
Assessment for RADARSAT 2 polarimetric modes

Maureen L. Yeremy, André Beaudoin,
Jonathan D. Beaudoin and Gillian M. Walter

Defence R&D Canada

National   Défense
Defence   nationale

Canadä

20020103 075

Global shoreline mapping from an airborne polarimetric SAR:

Assessment for RADARSAT 2 polarimetric modes

Maureen L. YEREMY, André BEAUDOIN,
Defence Research Establishment Ottawa

Jonathan D. BEAUDOIN,
Res. Student at DREO, Now at Univ. of NB, Fredericton, NB

Gillian M. WALTER,
Atlantis Scientific Inc.

Defence Research Establishment Ottawa

Abstract

A project between two agencies, the Defence Research Establishment Ottawa (DREO), Canada and the National Imagery and Mapping Agency (NIMA), USA, was initiated in 1998 to study shoreline extraction from imagery. NIMA's investigation involved Landsat imagery while DREO researched Synthetic Aperture Radar (SAR) applications with an emphasis on RADARSAT products. The focus of this report is the extraction of shorelines from polarimetric SAR imagery in preparation for the launch of RADARSAT 2 scheduled for November, 2003.

The desired shoreline vector product, for this project, is the Mean High Water Line (MHWL). This specification implies that further consideration of tidal models are required. For extracting MHWL estimates from imagery, tidal models must be referenced to surveyed positions with good elevation accuracy. Therefore, in addition to radar considerations, geomatics, topographic and oceanographic issues are included in this study. With sufficient tide and shore topography information, an image extracted waterline estimate can be improved to a MHWL.

Polarimetric SAR image data, with attributes similar to the future RADARSAT 2 specifications, were acquired from an airborne platform and exploited here to extract shorelines. Classification methods were used to detect the shoreline region. Contrast enhancement methods were implemented to emphasize the shoreline edge. The cross-polarized channels provided velocity information which was used for discriminating between non-stationary (i.e. ocean) and stationary surfaces (i.e. land). One method for extracting shore slopes was studied here to determine if it is feasible with C-band SAR data.

Two experimental trials acquired polarimetric SAR image data at both the high and low tide extremes. *In situ* ground truthing data were collected while the image data were acquired. The trial locations were the Bay of Fundy, Nova Scotia (NS), and the North Carolina (NC) coast. At NC, two separate sites were studied. Comparisons were made with either Global Positioning Systems (GPS) vector data collected along the mean waterline during the acquisition time, or a surveyed MHWL vector estimate.

Phenomenological differences between the shore types were observed and are documented here. One method to extract shore slopes was studied. This method did not produce reasonable results for the North Carolina site, but the Fundy results were near the expected values. Further research with sufficient ground truthed data is required to validate these Fundy shore slope results. Two different methods were used to estimate the mean error of the estimated vector shoreline relative to a reference shoreline. One method's mean error estimates varied between 0.2 and 10.5 m for all shorelines analyzed here. The other method's mean error estimate, between an image extracted waterline (at low tide) and a surveyed MHWL, was 6.3 m (6.8 m for the former method) over 2 km where the measurement uncertainty is about 7.0 m. In general, all image waterline estimates when compared to reference waterlines had average errors near the measurement uncertainty, and maximum errors of about 30 m.

Résumé

En 1998, deux organismes, le Centre de recherches pour la défense Ottawa (CRDO) du Canada et la National Imagery and Mapping Agency (NIMA) des États-Unis, ont lancé un projet pour étudier l'extraction de la ligne de rivage par imagerie. L'étude de la NIMA portait sur l'imagerie Landsat tandis que le CRDO a effectué des recherches sur des applications radar à synthèse d'ouverture (RSO), en portant une attention particulière aux produits RADARSAT. Le point central du présent rapport est l'extraction de lignes de rivage par imagerie RSO polarimétrique en préparation au lancement du RADARSAT 2 qui aura lieu en 2003.

Pour le présent projet, le produit désiré du vecteur de la ligne de rivage est le niveau moyen des hautes eaux. Cette caractéristique implique qu'il faut examiner davantage les modèles des marées. Pour l'extraction d'estimations du niveau moyen des hautes eaux par imagerie, il faut se référer aux modèles des marées pour évaluer l'altitude des positions avec une bonne précision. Par conséquent, en plus des radars, nous avons abordé des questions géomatiques, topographiques et océanographiques dans la présente étude. Une image extraite de l'estimation de la ligne des eaux peut être améliorée et convertie en niveau moyen des hautes eaux, si on dispose de suffisamment d'information sur la topographie des marées et du rivage.

Des données-image RSO polarimétriques ont été utilisées ici pour extraire les lignes de rivage. Nous avons utilisé des méthodes de classification pour détecter la région de la ligne de rivage. Des méthodes d'accentuation des contrastes ont été mises en œuvre pour intensifier la bordure de la ligne de rivage. Les canaux de polarisation croisée ont fourni des renseignements sur la vitesse; ces renseignements ont été utilisés pour faire la distinction entre les surfaces non stationnaires (c.-à-d., l'océan) et les surfaces stationnaires (c.-à-d., la terre). Une méthode d'extraction des pentes du rivage a été étudiée pour déterminer si c'était possible avec les données RSO de bande C.

Deux essais ont permis d'acquérir des données-image RSO polarimétriques pour les extrêmes des marées hautes et des marées basses. Des réalités de terrain *in situ* ont été recueillies tandis que des données-image ont été acquises. Ces données ont été recueillies dans la baie de Fundy, en Nouvelle-Écosse (N.-É.) et sur la côte de la Caroline du Nord. En Caroline du Nord, deux endroits différents ont été étudiés. Des comparaisons ont été effectuées entre des données de vecteur recueillies le long de la ligne moyenne des eaux avec des systèmes de positionnement global (GPS) lors du temps d'acquisition et des estimations de vecteur de niveau moyen des hautes eaux arpenté.

Nous avons observé des différences phénoménologiques entre les types de rivage; ces différences sont documentées ici. Nous avons étudié une méthode d'extraction des pentes de rivage. Cette méthode n'a pas donné de résultats satisfaisants pour l'endroit étudié en Caroline du Nord, mais les résultats pour la baie de Fundy se situaient près des valeurs prévues. Il faudra faire davantage de recherches et obtenir suffisamment de

réalités de terrain pour valider les résultats provenant de la baie de Fundy. Nous avons utilisé deux méthodes différentes pour évaluer l'erreur moyenne de la ligne de rivage sous forme vectorielle qui se rapporte à une ligne de rivage de référence. Les évaluations des erreurs moyennes par l'une des méthodes variaient entre 0,2 m et 10,5 m pour toutes les lignes de rivage analysées ici. L'évaluation des erreurs moyennes par l'autre méthode, entre une image extraite de la ligne des eaux (à marée basse) et un niveau moyen des hautes eaux arpenté, était de 6,3 m (6,8 m par l'ancienne méthode) sur 2 km alors que l'incertitude est d'environ 7,0 m. En général, toutes les estimations de la ligne des eaux à partir de l'image, comparativement aux lignes de eaux de référence, avaient des erreurs moyennes qui se situaient près de l'erreur d'incertitude, et des erreurs maximales d'environ 30 m.

Executive summary

Yeremy, M.L., Beaudoin, A., Beaudoin, J.D., Walter, G.M., 2000, 'Global shoreline mapping from an airborne polarimetric SAR: Assessment for RADARSAT 2 polarimetric modes', TR 2001-056, DREO.

Present day shoreline vector databases have large errors on the order of 500 m. This error is becoming less acceptable as other technologies improve. Other compelling reasons for improving these shoreline estimates include navigational, legal and disaster (e.g. tsunami flood prediction) issues.

Defence Research Establishment Ottawa (DREO) has researched the extraction of vector shorelines from Synthetic Aperture Radar (SAR) imagery for several environments. This report documents the results from this study which was in support of the Canadian Department of National Defence (DND) division, J2 Geomatics.

The National Imagery and Mapping Agency (NIMA), USA and J2 Geomatics both have a requirement to map North American and global shorelines at 1:250,000 scale. Hence, a Project Agreement (PA) between DREO and NIMA was made in 1998 to investigate the extraction of Mean High Water Lines (MHWL) from imagery. NIMA in collaboration with National Oceanic and Atmospheric Administration (NOAA) has researched this topic using LandSAT imagery while DREO studied shoreline vector extraction from SAR imagery. One part of the study involved commercial single channel SAR imagery. The other part, namely the work in this report, studied shoreline extraction from polarimetric SAR imagery. Although there are presently no commercial polarimetric space-borne SAR platforms, future satellites such as EnviSAT (expected launch in 2001) and RADARSAT 2 (expected launch in 2003) will provide dual and quad-polarimetric imagery.

In this report several polarimetric techniques were examined for this application. In order to extract a MHWL, other information such as tidal and geomatics data is required. From polarimetric imagery, information about the scatterer's structure, velocity and orientation can be determined for some conditions. In comparison, for most single channel SAR data, magnitudes are the only information available.

Two experiments involving well ground truthed polarimetric SAR imagery were conducted at North Carolina (NC) and Bay of Fundy, Nova Scotia (NS) regions. At NC, two sites, separated by a distance of 300 km, were studied: Duck and Camp Lejeune. Comparisons were made with either a surveyed MHWL vector estimate (Duck) or in situ GPS measured estimates (other sites). Single channel image data were sufficient for extracting shorelines which were distinct in the imagery. For more complicated shoreline imagery, where the backscatter from the waves and beach are comparable (e.g. Duck), the extra information from polarimetric data improved the results. All extracted shoreline (waterline) estimates (seven images studied) here had mean errors between 0.2 and 10.5 m, which were near the measurement uncertainty. Further research with polarimetric data is required to determine if shoreline slope information (and therefore MHWL estimates) for some environments can be obtained.

Sommaire

Yeremy, M.L., Beaudoin, A., Beaudoin, J.D., Walter, G.M., 2000, 'Global shoreline mapping from an airborne polarimetric SAR: Assessment for RADARSAT 2 polarimetric modes', TR 2001-056, CRDO.

De nos jours, les bases de données de vecteurs de la ligne de rivage présentent des erreurs importantes de l'ordre de 500 m. L'amélioration des autres technologies rend cette erreur de moins en moins acceptable. Il y a d'autres raisons pour nous convaincre d'améliorer ces estimations de la ligne de rivage, notamment la navigation, l'aspect juridique et les catastrophes (ex. : la prédiction des inondations des tsunamis).

Le Centre de recherches pour la défense Ottawa (CRDO) a effectué des recherches sur l'extraction de vecteurs de lignes de rivage par imagerie radar à synthèse d'ouverture (RSO) pour plusieurs environnements. Le présent rapport documente les résultats de cette étude, qui appuie la division J2 Géomatique du ministère de la Défense nationale (MDN).

La National Imagery and Mapping Agency (NIMA) des États-Unis et la J2 Géomatique ont toutes deux une exigence pour la cartographie de l'Amérique du Nord et des lignes de rivage du monde, soit d'utiliser une échelle de 1 / 250 000. Une entente a donc été conclue en 1998 pour étudier l'extraction du niveau moyen des hautes eaux par imagerie. En collaboration avec la National Oceanic and Atmospheric Administration (NOAA), la NIMA a effectué des recherches sur ce sujet à l'aide de l'imagerie LandSAT, tandis que le CRDO a étudié l'extraction du vecteur de la ligne de rivage par imagerie RSO. Une partie de l'étude portait sur l'imagerie RSO à monocanal commercial. L'autre partie, notamment les travaux présentés dans le présent rapport, a étudié l'extraction de ligne de rivage par imagerie RSO polarimétrique. Quoi qu'il n'existe actuellement pas de plates-formes commerciales RSO aéroportées polarimétriques, les prochains satellites, comme EnviSAT (lancement prévu en 2001) et RADARSAT 2 (lancement prévu en 2003), offriront une imagerie à polarimétrie double et quadruple.

Dans le présent rapport, nous avons étudié plusieurs techniques polarimétriques pour cette application. Afin d'extraire un niveau moyen des hautes eaux, nous avions besoin d'autres renseignements, comme des données géomatiques et des données sur les marées. Il est possible d'obtenir, par imagerie polarimétrique, des renseignements sur la structure, la vitesse et l'orientation du diffuseur pour certaines conditions. Par comparaison, pour la plupart des RSO à monocanal, les données relatives à la grandeur sont les seuls renseignements disponibles.

Deux expériences concernant l'imagerie RSO polarimétrique des réalités de terrain ont été menées en Caroline du Nord et dans la baie de Fundy, en Nouvelle-Écosse (N.-É.). En Caroline du Nord, deux endroits, situés à 300 km l'un de l'autre, ont été étudiés : Duck et Camp Lejeune. Des comparaisons ont été effectuées entre une estimation du vecteur du niveau moyen des hautes eaux arpenté (Duck) et des estimations mesurées *in situ* avec un GPS (autres endroits). Des données-image à monocanal ont été

suffisantes pour extraire les lignes de rivage qui étaient distinctes dans l'imagerie. Pour une imagerie de ligne de rivage compliquée, lorsque la rétrodiffusion des vagues et de la plage sont comparables (ex. : Duck), les renseignements additionnels tirés des données polarimétriques ont amélioré les résultats. À Duck, des estimations très raisonnables ont été obtenues, avec une erreur moyenne, sur plus de 2 km, d'environ 6,3 m entre le niveau moyen des hautes eaux et une ligne des eaux de marée basse extraite (c.-à-d., le pire cas). Toutes les estimations de ligne de rivage (ligne des eaux) (sept images ont été étudiées) avaient des erreurs moyennes qui étaient inférieures à 10,5 m. Il faut effectuer d'autres recherches avec des données polarimétriques pour déterminer s'il est possible d'obtenir des renseignements sur la pente de la ligne de rivage (et par conséquent, des estimations du niveau moyen des hautes eaux) pour certains environnements.

Table of contents

List of figures

List of Tables

Acknowledgements

1. Introduction

A global shoreline database had previously been compiled by National Imagery and Mapping Agency (NIMA). These results were based primarily on photogrammetry techniques using air photographs and maps. The detected vector shorelines were extracted from debris lines visible in the photographs and provided reasonable estimates within 500 m error limits for 90% of all shorelines. For present day operational requirements these estimates are not acceptable. More accurate shoreline vectors are required for many reasons including, mapping, navigation, and flood predictions. Because of these requirements a collaborative study between NIMA and Defence Research Establishment Ottawa (DREO) was initiated to determine if accurate shoreline estimates can be obtained using present day imagery.

DREO investigated shoreline extraction applications using Synthetic Aperture Radar (SAR) imagery. This report is the second portion of a two part study. The first part's focus is on applications using RADARSAT and other space-borne, single channel SAR imagery [1]. This second part is devoted to studying applications for polarimetric SAR imagery in preparation for the launch of two satellites, EnviSAT and RADARSAT 2 (scheduled for 2001 and 2003 respectively), which will have dual and quad-polarization modes.

Shoreline extraction from imagery has previously been studied [Refs. 2, 3, 4, 5, 6, 7]. These studies have confirmed that shoreline vectors can be detected from imagery within limitations. Shoreline extraction studies would benefit further, however, from research which determines what physically are these edges in the imagery since they are not necessarily the *in situ* waterline and are dependent on different phenomenology. In this study, at each study site, ground truthing was conducted during the acquisition time in order to validate the interpretations and results.

Shorelines are usually well defined in most image types as an edge between two contrasting regions, near the land-water interface. One image type, C-band SAR, which is the data type studied in this project, is particularly optimal for distinguishing this edge.

This project's desired end product is to develop a method for extracting a Mean High Water Line (MHWL) vector estimate from imagery. By definition, MHWL is the horizontal vector shoreline determined at an elevation which is the mean of the maximum high tide elevations over nineteen years. The distance between MHWL and the *in situ* waterline is dependent on the tidal stage and the daily tidal variability. For the worst case, at low tide, the distance is small (large) for steep (shallow) shore slopes. Capturing an image near high tide usually reduces this error. However, high tide elevations are seasonal and can be quite variable. Also, perturbations from tidal models occur regularly due to environmental conditions. For a project like shoreline mapping the logistics of acquiring satellite images at the local high tide could also be very difficult. Instead, if more accurate shorelines are required, a waterline estimate can be improved to a MHWL estimate, provided the appropriate information is

available. In particular, the shore slope and a tidal model, which is geo-referenced (with accurate elevation information), is required. If possible, local tidal elevations at the acquisition time would also improve the estimate and remove errors caused by temporal variability.

1.1 Study context

For this study, polarimetric image data were collected from several different types of environments. During the SAR data acquisition, ground truthing was conducted so that extracted waterlines could be validated with *in situ* measurements. Contrast enhancement methods were implemented for accentuating the land-water edge in an image. A procedure was developed for extracting shorelines from these enhanced image data. One method to extract shore slope information was studied. Shore slope data potentially can improve a shoreline estimate to a MHWL estimate.

For accurate MHWL estimates, tidal models referenced to chart datum positions must be included in the study. The addition of *in situ* tidal elevation data at the image time would also improve the results. This implies that a coordinated effort is required to accomplish this. A major obstacle to this project is that current world tidal model databases are not well maintained nor are they reliable. For this project, improving tidal models and referencing them to elevations should be a consideration of this project [8, 9]. Realistically, incorporating tidal information may not presently be feasible, but it should be considered for future efforts particularly since global environmental data, positioning data and image exploitation capabilities are constantly improving with time.

1.1.1 Shoreline delineation requirements

Several government agencies world-wide have a requirement for accurate shoreline estimates. The delineation of the shoreline is important for legal and mapping responsibilities, and it is also useful for Digital Elevation Mapping (DEM) projects which require masking water bodies in order to ameliorate topographic mapping errors. A vector shoreline database is also useful for disaster predictions and military and peace keeping operations where assessment of an environment is required for logistics and damage control.

Both Canada and the United States have a requirement to update their internal topographic and shoreline databases. This project's results will hopefully assist updating these databases. In the future, as capabilities such as shoreline extraction improve, then, space surveillance projects which monitor dynamic environmental processes (e.g. such as shoreline erosion, opening of the North-West passage), conceivably will be possible.

1.1.2 NIMA / DREO Joint Project

NIMA (USA) and DREO (Canada) have a mandate to provide better shoreline estimates both internally and abroad. Because of this they began a collaborative project to explore space-borne image applications for the extraction of shoreline vectors. A two year Project Agreement (PA) between NIMA and DREO began in late 1998. The study documented here is the outcome of this initial agreement.

Several sites were studied for this project and they include the MacKenzie Delta in the Canadian arctic, the Bay of Fundy, Nova Scotia, Canada and the North Carolina, USA coastline at Duck and Camp Lejeune. Polarimetric data were only acquired at the Fundy and North Carolina coastlines and these data are documented in this report. The MacKenzie Delta results and single channel SAR results are documented in [1]. A final collated report [10] will compile all NIMA, NOAA and DREO's contributions and compare all shorelines for the Duck, NC site.

1.2 Shoreline objectives

In this report, the objective is to evaluate how well polarimetric data and applications (a) distinguish the waterline and other features in the littoral region and (b) provide sufficient information for improving the waterline to a MHWL estimate. Ground truthed data are used in this study for validation.

The experiment involves several parameters, as demonstrated in Figure 1. In particular, if a shore slope estimate, ζ', can be determined, then with sufficient tidal knowledge the elevation difference, $\hat{z}$, between the elevation of the MHWL and *in situ* waterline provides a distance which can be projected onto the shoreline. This projected vector provides a MHWL estimate and requires four types of information: (1) shore slope, (2) tidal model for the region, (3) reference surveyed positions relative to the tidal model, and (4) waterline elevation at the image time. The last data type can be calculated from the tidal model. However, these calculations are not accurate due to tidal temporal variation.

It is unlikely that reasonable MHWL estimates can be made for most shorelines within the near future, since most of the world's tidal statistics and elevations are either unknown or inaccurate. However, with projects such as Topex Posiedon, global tidal models are in the process of being improved. Satellite (image and position) and Global Positioning Systems (GPS) data quality and accuracies are also improving.

More accurate MHWL extraction methods are only possible if tidal reference points are surveyed with good elevation accuracy as proposed by O'Reilly and Parsons [8, 9]. This is now possible because of accurate GPS data, but requires national and world-wide commitment and support. Because space-borne imagery and GPS are all in geodetic coordinates (i.e. WGS 84), referencing shoreline and tidal information to the same coordinate

system would be the most suitable, and would reduce the number of coordinate transformations required. An investment in surveyed tidal data collected world-wide would complement several applications, such as navigation, tsunami predictions, rising sea levels and flood events.

In this study, polarimetric methods are exploited to determine whether polarimetric data and applications provide better results relative to single channel SAR data, other applications (e.g. InSAR) or other image types. There have not been sufficient tests for all types of shore environments and this should be considered for any future applications or studies.
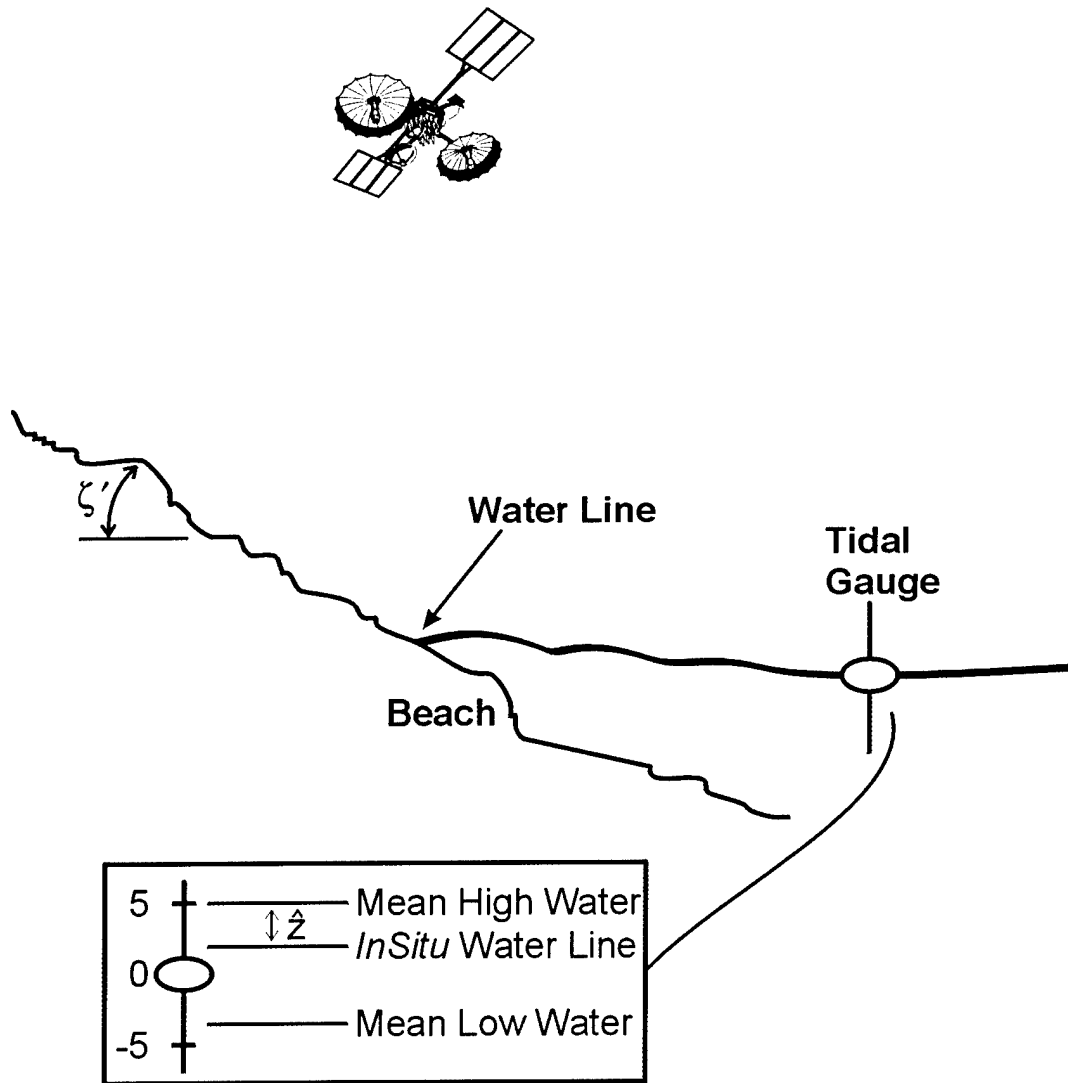
Figure 1. Parameters required for shoreline mapping are shown here and are discussed further in Section 1.2.

1.3 Shoreline mapping using space-borne SAR data

Space-borne SAR and other image types are used increasingly more for mapping projects because of several reasons, including logistics and economics. The advantage of SAR over other image types is that these data are not limited by cloud cover or night-time conditions. C-band SAR (e.g. RADARSAT) is an optimal band for distinguishing land from water since the backscattered difference between these two surfaces are usually at least an order of magnitude. This is due, in part, to specular reflection from the somewhat flat ocean surface with the exception of Bragg scattering effects from ocean surface capillary waves modulated by long gravity waves.

Although there are inherent geo-referencing problems with SAR for regions where topographic variations are large, the errors for flatter regions are generally not significant for many mapping accuracies (e.g. 30 m postings). This study pertains to regions where topographic variations are small. Geometric corrections with a terrain map may be required for regions with moderate topographic change (e.g. 15 – 30 m elevation change) while regions with significant topographic variations would likely require methods such as Interferometric SAR (InSAR) or stereo applications.

For this project the desired vector is the MHWL within an error limit of about 30 m. Capturing a waterline from imagery introduces an error which is dependent on the shore slope and tidal elevation variations. Provided the shore slope is not shallow, the horizontal discrepancy between low and high waterlines is often within most mapping error limits. For instance typical daily tidal elevation differences of 2 m for a 7° shore slope represents a maximum horizontal error of about 16 m which is within this project's mapping limitations. However, for shallower slopes, the error from the MHWL can be quite large, and corrections such as proposed here, should be considered.

1.3.1 RADARSAT 2 : Polarimetric SAR Imagery

This report documents a shoreline extraction study in preparation for the polarimetric modes of RADARSAT 2.

RADARSAT 2 will have many of the standard modes of operation that RADARSAT now has, except that some modes will have smaller resolution sizes (e.g. 3 m). The frequency will be slightly different but still C-band. In addition, RADARSAT 2 will have a couple of modes which are fully polarimetric at pixel sizes similar to RADARSAT's fine beam mode (~9m) and standard beam mode (~25m). There also will be the option for several dual-polarization modes (i.e. HV-HH and VH-VV). One other advantage RADARSAT 2 will have relative to RADARSAT is that it will have both right and left looking capabilities.

For this project, we obtained polarimetric SAR data from an airborne system with a centre frequency and data acquisition method similar to RADARSAT 2. The results presented here are an indication of RADARSAT 2 capabilities. RADARSAT 2 however, will be built at a more technologically advanced time than this airborne system.

1.3.2 Polarimetric SAR: Introduction

Below is a brief introduction to polarimetric data and its attributes.

An elliptical electromagnetic wave propagating from a transmitter along the z axis or Line of Sight (LOS) can be described as

$$E^{tr} = E_v^{tr}\hat{v}_{tr} + E_h^{tr}\hat{h}_{tr}$$

in the plane perpendicular to the axis as shown in Figure 2. Here, for a transmitted wave (denoted by 'tr'), $E, \hat{h}, \hat{v}$, represent the electric field, and unit reference coordinates in the plane perpendicular to the propagation direction. For a monostatic system, the backscattered wave (denoted by 'sc') is related to the transmitted wave by,

$$\begin{bmatrix} E_h^{sc} \\ E_v^{sc} \end{bmatrix} = \tilde{S} \begin{bmatrix} E_h^{tr} \\ E_v^{tr} \end{bmatrix},$$

and $\tilde{S}$, the scattering matrix is described as,

$$\tilde{S} = \begin{bmatrix} S_{HH} & S_{HV} \\ S_{VH} & S_{VV} \end{bmatrix},$$

using the Back Scattered Alignment (BSA) convention [11, 12]. Since polarimetric data provides four channels compared to single channel data, the span, which is the sum of the power from these four channels, implies greater Signal to Noise Ratios (SNR) relative to single channel power. From $\tilde{S}$, the orientation, ψ, and ellipticity, χ, can also be determined. Here, the ellipticity angle at $0°$ ($45°$) defines linear (circular) polarization.

Applications for single channel data have relied on the statistics and texture of these data. One advantage of polarimetry is that statistical and texture information is available for four channels. From decomposition methods, structural and orientation information can also be obtained. Target decomposition methods have been developed in order to identify structure types [13, 14, 15]. These type of applications are suitable for very reflective targets which have well defined shapes. A composite of several scatterers and their spatial distribution in the imagery could potentially classify a target [16]. In contrast other decomposition methods utilize statistical moments and distributions in order to categorize a relatively homogeneous region such as land or ocean clutter [17, 18, 19].

Coherence (or correlation) methods between the HV and VH channels can be implemented as a measure of velocity [20] which can be used to distinguish moving objects (ocean) from stationary objects (land). Fitch [21] introduced this concept for single channel data. Fully polarimetric data, however, by virtue of the processing method has this capability readily available. This application is possible because by the reciprocity theorem [22],

$$S_{VH} = S_{HV}$$

for environments where Faraday rotation is not relevant (often the case). The perception that this relationship is violated occurs for fully polarimetric SAR imagery due to the acquisition method. Most polarimetric SARs transmit the horizontal and vertical component alternately. For each transmitted signal, both channels (H and V) are received. By doubling the Pulse Repetition Frequency (PRF) the two transmitted data sets (H and V) can be oversampled so

that their discrete spatial samples in the azimuth are the same. Consequently the cross channels, HV and VH will not be sampled at exactly the same time, and therefore, will not equal each other for cases where either spatially the topography has changed or temporally the scatterer has moved during the imaging time. This phenomenon is very similar to along-track InSAR and is useful for distinguishing regions where motion occurs (e.g. ocean waves, trees blowing in the wind). This velocity information can be useful for distinguishing large ocean backscatter regions from land regions. For this shoreline project, it is used for extracting waterlines and distinguishing between large tidal waves, offshore islands or sand bars. This method is not as accurate as along-track InSAR, and it cannot distinguish changing topography from velocity. This same effect, alternatively, can be achieved using single channel data [21] with extra effort and provided the platform's PRF can be doubled. Polarimetric data from systems such as Jet Propulsion Laboratory's (JPL) AIRSAR do not have separate HV and VH channels and therefore cannot implement this approach.
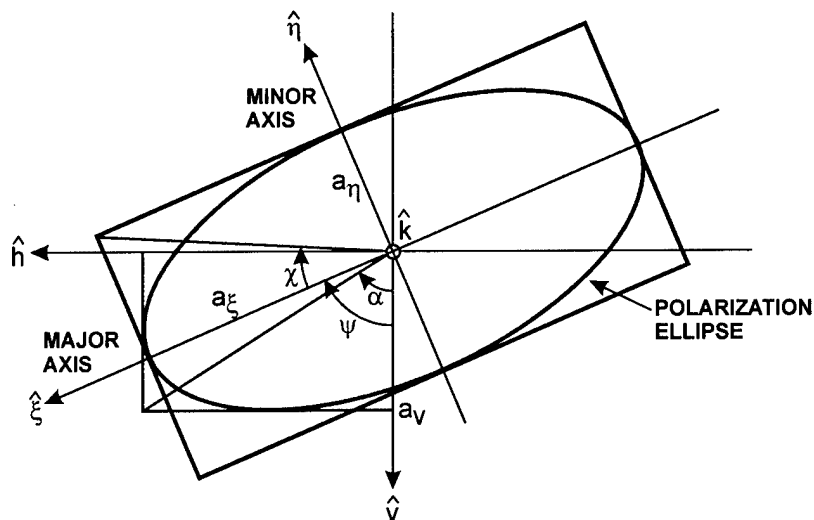
Figure 2. Here the electromagnetic wave is shown projected onto the h-v plane while it is propagating in the k direction (for a monostatic system it is either in or out of the page depending on whether it is a transmitted or received signal). The ellipse is rotated at an orientation angle of ψ from the v axis to the ξ-η reference frame which is aligned with the elliptical major and minor axes. The ellipticity angle, χ (relative to the ξ axis) is zero for linear polarization and forty five degrees for circular polarization. The ellipse components 'a' are notated here for each axis

1.4 Report structure

DREO's project involvement included two types of image data: (1) single channel SAR data (RADARSAT predominantly), and (2) airborne polarimetric SAR data (in preparation for RADARSAT 2). The first part of this project will be reported in [1] (in progress), where further details and information about each experiment and data type can be found. This report discusses polarimetric data and analysis results only. The Data (polarimetric SAR and ground truthing), and Analysis are documented and are followed by a discussion of the Results and Conclusions.

2. Shoreline mapping : polarimetric SAR data

This section is divided into two subsections. One subsection discusses the ground truthing emphasizing the phenomenological differences at each site, while the other subsection discusses the SAR data collection and quality.

2.1 Data : Test sites and ground truthing

Polarimetric image data from the two regions: the Bay of Fundy and the North Carolina coastlines were acquired while ground truthed data were collected. Airborne SAR missions at both low and high tides acquired several image lines at each site. A discussion below compares the different environments and corresponding SAR responses. Environment and ground truthing descriptions for each site are also documented.

2.1.1 Shore types : phenomenology in SAR

Physical oceanographers often classify beach types by interrelating characteristics such as beach particle size and distribution, wave energy, prevailing winds and tidal dynamics [23, 24, 25]. For example, beaches where energetic waves are common, are often characterized with a steeper foreshore region and large particle sizes (pebbles or coarse sand), which are graded by increasing size with higher elevations. In contrast, fine particle sediments and shallow slopes are generally found on beaches where the waves are commonly mild. The two sites studied here are phenomenologically different. The NC beach is much like the former description with energetic wave action while the Bay of Fundy is similar to the latter description with weak coastal waves. The SAR image responses for these two shore environments are different also, despite the shoreline commonality.

The Bay of Fundy is a region where some of the largest tides in the world occur. It is in a protected bay (Figure 3) where the tidal currents are relatively subdued compared to exposed ocean areas. The beach material is graded from very fine particles in the foreshore region to sand and then gravel in the upper shore regions. Figure 4 contains several photographs which show characteristics of the shoreline at the Bay of Fundy. In Figure 5, a SAR image of the Bay of Fundy is overlaid with a ground truthed waterline vector (in yellow) collected at a high tide near the date of the image acquisition. These waterlines are very near the well defined demarcation between land and water observed in the imagery.

In contrast, Duck, NC (Figure 6) is a very exposed region where large dynamic waves play an active role in shoreline erosion. The beach material is very coarse, large flaked sand and the beach slopes are much steeper compared to the Fundy beach. In the Duck images, the waterline is not as distinct as for the Fundy coast because the backscatter from the wave structures are greater or comparable to the local beach surface. The backscatter from the beaches are small and it is speculated that this is due to volume scattering losses from the very

coarse sand flakes once the electromagnetic wave penetrates the surface. An alternate explanation could be from specular reflection, but this seems unlikely since the Duck surface
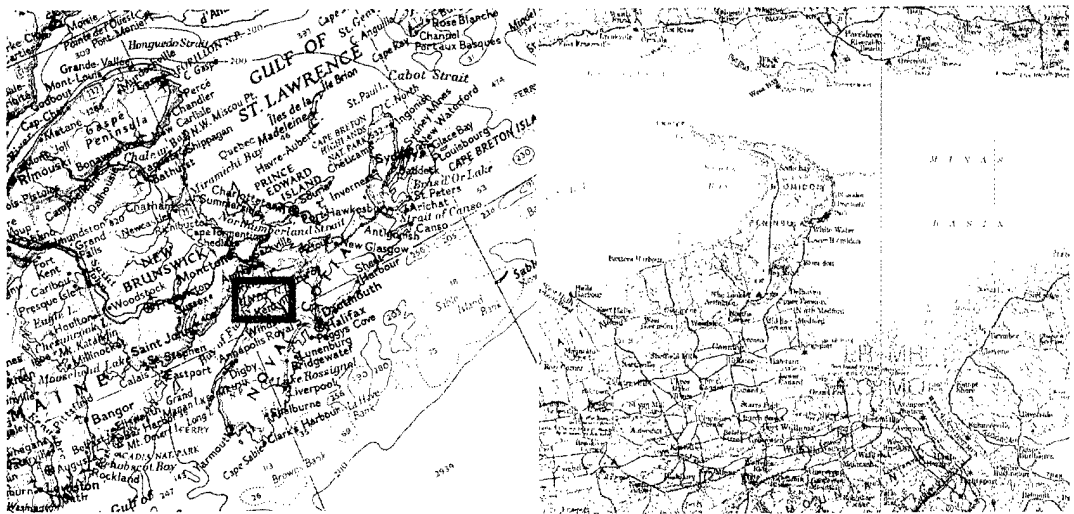
Figure 3. Bay of Fundy. The map to the right is a close-up of the area found in the pink rectangle on the map to the left.

Figure 4. Photographs of the Bay of Fundy at low (upper and lower right) and high (lower left) tide.

DREO TR 2001-056
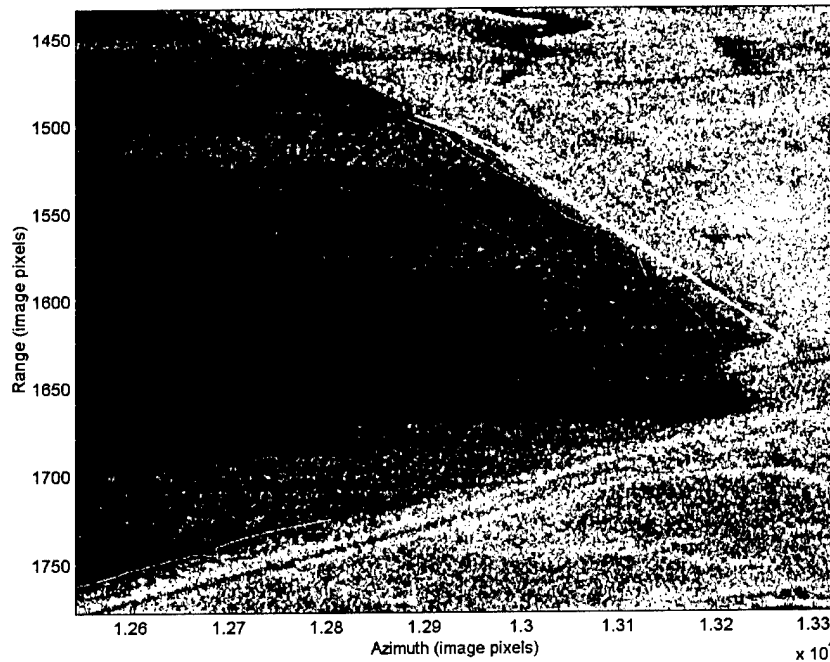
Figure 5. The Bay of Fundy. The yellow line is a GPS ground truthed high tide measurement collected in both directions (i.e. up and down shoreline). The axes are in image coordinates with range and azimuth lengths of ~1.7 km and 350 m. The Red, green and blue image composite represent the HH, HV and VV components. White (black) represent high (low) backscatter.
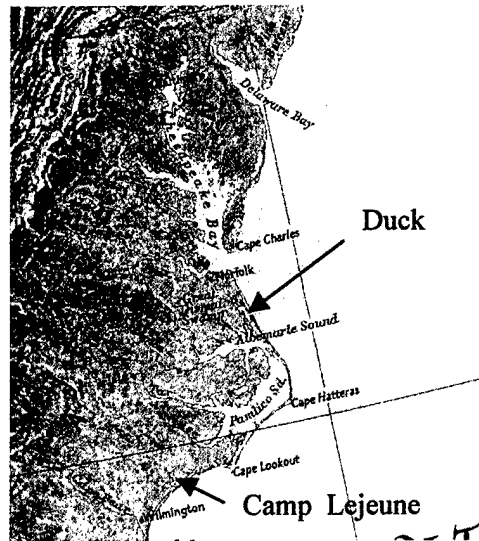
Figure 6. North Carolina. Data were acquired for two sites in North Carolina for this report: Camp Lejeune and Duck.
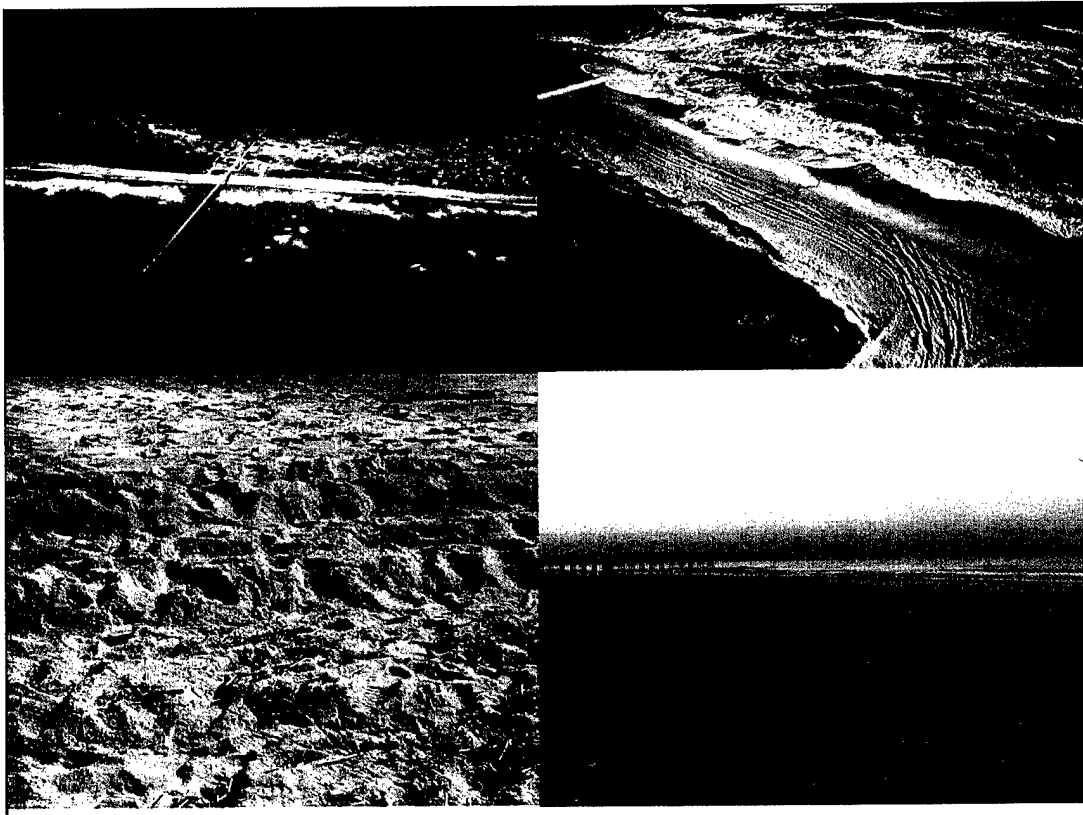
Figure 7. Photographs at Duck and Camp Lejeune, NC. Upper left is an overhead view of Duck, NC. Note the large tidal waves, pier and buoy array to the right of the pier. Upper right is a close-up of Duck's beach. Note the vegetated sand dunes, tracks in the sand and large waves. Lower left is an example of the coarse sand found on NC beaches. Lower right is the beach at Camp Lejeune with a wooden pier.

was rough compared to the Fundy coast. As seen in Figure 8, the detection of the waterline is not a simple matter of extracting the waterline from an edge with high contrast, since there are several edges associated with the incoming waves and the vegetation line. The dark beach (i.e. low backscatter) is "sandwiched" between two bright (i.e. high backscatter) regions, the waterline and vegetated land. This dark beach could easily be confused with the ocean, if the logic used for the Bay of Fundy (i.e. ocean is dark and land is bright), was implemented instead. This demonstrates the requirement for ground truthing each different type of environment.

Other problems associated with the detection of beach environments from imagery are related to the movement from currents and wave features while the SAR data is acquired. This can create distortions in the SAR image and is discussed further in the results.
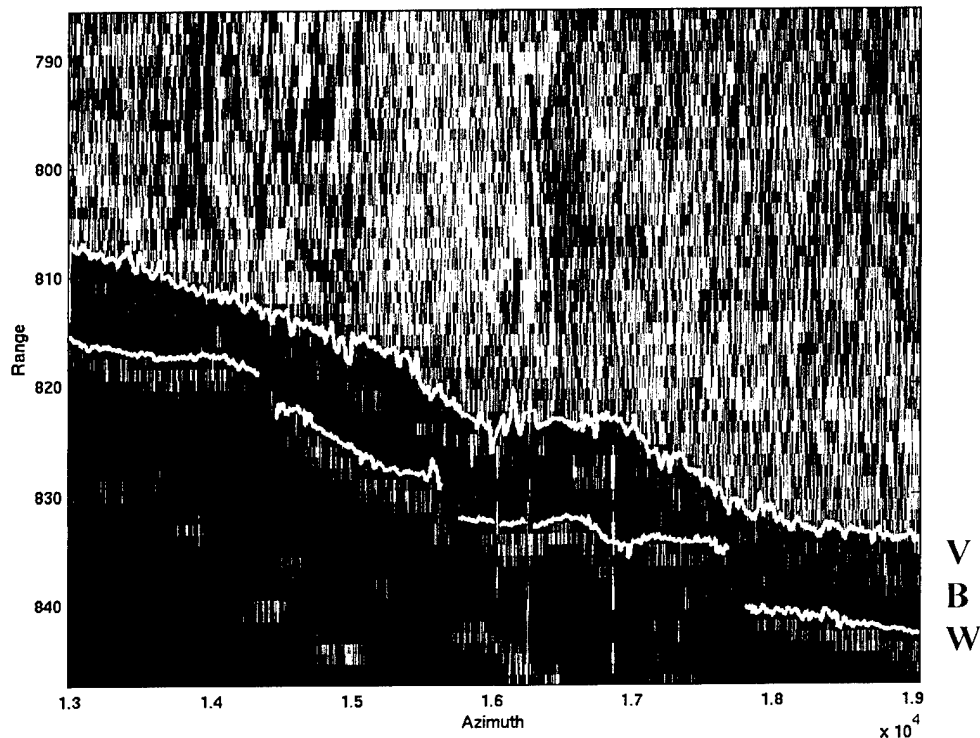
Figure 8. Vector segments in white delineate the extracted vegetation and waterline at Duck, NC. The background is an image after the Pre-Whitening filter and weight have been applied. The vegetated line (V), beach (B) and waterline (W) are labelled in red. The axes are in image pixel co-ordinates for range and azimuth lengths of about 350 m and 2.4 km.

2.1.2 Bay of Fundy, NS : site and ground truthing

The Bay of Fundy region (Figure 3) is a protected coastal region with gently rising tides, and shallow shore slopes. The beaches are very fine clay-sand with particle size gradations increasing to gravel near the debris line. The study area is a combination of rural and natural environment settings.

Image data were collected in November, 1998 for the Bay of Fundy region at Scots Bay, Blomidon Peninsula and Five Islands, Nova Scotia, Canada. Phenomenologically all of these sites are different. Scots Bay has a very shallow sloped beach where the low tide extends kilometres from the high tide waterline. Blomidon is an area where there are steep cliffs with a narrow shore. The Blomidon cliffs taper off to an area where another shallow beach region exists. The Five Islands are rocky eroded islands with steep cliffs which punctuate the ocean at high tide or shallow beach at low tide. This region experiences the largest tidal variations

in the world. For this study, only Scots Bay was studied. The other two sites are better analyzed using InSAR or stereo pair methods which require at least two images. These methods are preferable for regions with considerable topographic variations because of SAR attributes like shadow and lay over.

The SAR was flown at low and high tide on flight lines which were parallel and perpendicular to the shoreline. Each mission began near the tidal peak time and lasted for about 1.5 hrs. Unfortunately, all the Bay of Fundy data were lost except for one flight at high tide due to data recording and in-flight communication problems. The results from this one flight (line 2 pass 1, Nov 23, 1998 at high tide) are reported here. Another data set which was flown in the same region the following year (low tide scene, line 4 pass 1, Nov 10, 1999) was used to study one of the analysis techniques.

In situ ground truthing using a GPS receiver mapped the waterlines within about an hour of the SAR flight time and tidal peak (i.e. high or low tide). The surf zone was mapped from a helicopter platform at about 100 ft altitude using a laser range finder attached to the GPS receiver. This GPS waterline measurement is compared here with the extracted waterline. The flight was very smooth, despite high wind conditions while the laser range finder was aimed at the shore surf zone during SAR acquisition times. For these altitudes, the horizontal GPS measurement error is estimated at about +/- 4 m. The fluctuating tidal waves at this time introduced another error of about +/- 4 m. Ground Control Points (GCP), used for georeferencing the images, introduced another error of +/- 5 m resulting in a total experimental error of about 7.5 m. The GPS receiver lost satellite contact for parts of the positional data collection over the waterline, resulting in data gaps. For the Fundy experiment, GPS measurements were also collected at the high tide waterline the previous day along the shoreline (back and forth trip took about 70 minutes). Within this time period, the high tide edge did not change significantly within the elapsed time as can be seen in Figure 5. Ground truthing of the beaches also included mapping the interface regions between different surfaces (e.g. gravel, sand, clay, rock).

For some of the Fundy coastlines, the distance between Mean Low Water Line (MLWL) and MHWL can be as great as 2 km because of the shallow slopes. Therefore, for this region knowledge of the shoreline slope is more critical for determining the MHWL than many other shorelines.

Although the image data at low tide was lost due to a malfunctioning data recording system, a real-time image was produced during the flight time. This image revealed a visible line near the low tide waterline and near the high waterline, which it is speculated could likely be extracted if the data were available. These two lines occurred where there was a transition to a very low backscatter region at the Fundy mud flats. It is speculated that this low backscatter response is because this is an extremely smooth, flat surface since the mud at Fundy has a plastic like consistency which returns to a very flat profile after deformed. Therefore much of the radar return would be reflected specularly, resulting in greater contrast at both sides of the mud flat (i.e. near the high and low tide waterlines). If the waterline could be extracted, then a MHWL could be estimated if shore slope information could also be extracted. Since low tide data were lost, we have studied another site near the Bay of Fundy (from Nov, 1999) to determine if shore slopes can be extracted from these type of smooth mud flats.

2.1.3 North Carolina, USA : site and ground truthing

The coastal North Carolina study sites are exposed beaches with moderately steep foreshore slopes and very coarse sandy beaches. This is an area where significant erosional effects occur due to the energetic wave action. Two coastal regions were studied in North Carolina: Duck and Camp Lejeune (Figures 6 and 7). Camp Lejeune's beach is mostly a natural beach with a few buildings while Duck is an urban environment pocketed between a natural beach environment. Both locations have a pier extending from the beach. Both sites' beaches were predominantly composed of coarse sand. Parallel to the shoreline and on the land side of the beach were eroded sand dune cliff edges (about 2m high). The dune edge marked the beginning of vegetated growth relative to the shoreline.

The imagery studied here were collected 2 weeks after Hurricane Floyd (September 1999) passed through the area. Bathymetric data collected before and after this storm changed slightly (data obtained from Duck's Field Reseach Facility web site) and may account for some small differences between these and other reference shorelines (e.g. MHWL survey) which were collected after this data acquisition.

Light Detection and Ranging (LIDAR) data were collected at both sites and is used as a form of ground truthing since it provides topographic and bathymetric information for the nearshore, backshore and adjacent beach areas. There are shoreline extraction methods for LIDAR data also and these results will be compared in [10].

A surveyed MHWL was collected at Duck a few weeks after the image data acquisitions. This estimate was based on a one year tidal average, was conducted by NOAA [10] and is compared with the extracted shorelines presented here. A method for calculating error estimates was specified by NIMA and is described in Ref. 10; this method was used to compare all shoreline results from different imagery. An error estimate for the worst case (i.e. between the Duck MHWL estimate and a data acquisition at low tide), is presented here.

In situ ground truthing information was collected for these imagery and included mapping the waterline and shoreline features with a differential GPS system (Trimble, experimental error of about 1 m). Contributing errors included: the spatial accuracy for georeferencing Ground Control Points (GCPs) in the image is about 5 m and the waterline variation during the acquisition time is estimated at about +/-4 m. This results in an experimental error of about 6.5 m for the extracted shoreline vector estimate. During the acquisition time, other ground truthing measurements included: soil moisture, wind direction and speed measurements, and mapping topographic, man made and interface regions for the beach, sand dune and vegetated land regions.

2.2 Data: Airborne polarimetric SAR

The data analyzed here were collected with Environment Canada's Convair CV-580 airborne SAR system which was developed by the Canada Centre for Remote Sensing (CCRS) [26]. The data were fully polarimetric C-band data. Sample sizes are 4 m in slant range and about 40 cm in the azimuth direction.
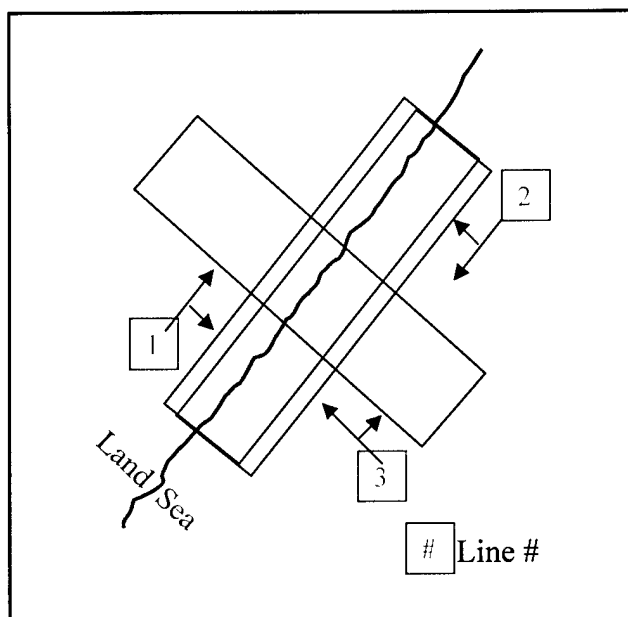
Figure 9. Airborne tracks at Camp Lejeune, NC. The arrows from the line numbers indicate the airplane's heading and SAR look direction.

The data were processed and calibrated using methods developed by CCRS [27]. Quality control tests indicated that the data had good relative calibration.

For each of the experiments, calibration equipment included at least one corner reflector and one Active Radar Calibrator (ARC). Calibration data were taken near the experimental sites within two hours from the image acquisition time.

In Figure 9, the tracks for the Camp Lejeune trial are shown. Line 1 and 2 are flown parallel to the beach while line 3 is flown perpendicular to the beach. This was a typical flight plan for all of the different sites (i.e. Fundy, Duck and Camp Lejeune).

Many of the image data sets had spectral leakage problems from the land into the water which can be observed as bright streaks extending from the shore into the ocean. This is likely due to saturated data associated with the fact that the data is stored digitally in range-compressed form. Also, Signal Timing Control (STC), which is a range-dependent gain correction, is not applied in the real-time processing. Consequently, it is more difficult to determine proper gain levels during the image acquisition, which can result in data saturation [28], particularly when the near field is ocean and not land. Since the data is stored in range compressed form, the original data cannot be reprocessed with a more suitable gain. For the shoreline experiment it is particularly difficult to avoid this problem, since the dynamic range between land and water is large. These data acquisition problems should not be significant in future SARs such as RADARSAT2.

Many of the Duck image lines had severe spectral leakage problems, which may be because it is the most urban site studied for this project. Line 6 pass 1 had the best quality image from

Duck. The line 8 pass 3, Duck acquisition is a low tide scene where the SAR was flown nearly perpendicular to the beach. This image is suitable for determining the shore slope. Unfortunately image streaks due to saturation were very severe for this image. The waterline vector and shore slope extraction processes were difficult to obtain because of these streaks. This was found to be predominantly due to spectral leakage problems near the shoreline region. Other modifying factors include the SAR response to wave motion [29]. The Camp Lejeune image lines had less spectral leakage problems compared to the Duck data.

Multiple polarimetric SAR images were collected near the high and low tide times at each site. Four lines were processed and calibrated from the Duck acquisitions (Oct 3, 1999) based on uncalibrated, real-time images. These are: line 7 pass 2 (collected at both low and high tide), line 6 pass 1 (low tide) and line 8 pass 3 (low tide). At Camp Lejeune (Oct 4, 1999), two calibrated lines (line 1, pass 1 and line 2, pass 2) at low tide were analyzed. Only one high tide data scene was available from Fundy (Nov 23, 1998, line 2 pass 1). Low tide data collected in the Fundy region in the following year was used for one application (Nov 10, 1999)

Table 1 below, indicates all of the data processed, calibrated and analyzed for this study.

Table 1. **Image data analyzed for this study.**

DATE	SITE	LINE #	PASS #	TIDE	COMMENTS
Nov23/98	Fundy, NS	2	1	High	Data quality good
Oct 3/99	Duck, NC	6	1	Low	Data quality good
Oct 3/99	Duck ,NC	7	2	High	Spectral leakage / unknown signal in noise data
Oct 3/99	Duck, NC	7	2	Low	Spectral leakage
Oct 3/99	Duck, NC	8	3	High	Spectral leakage / unknown signal in noise data
Oct 4/99	Camp Lejeune, NC	1	1	Low	Data quality good
Oct 4/99	Camp Lejeune, NC	2	2	Low	Data quality good
Nov 10/99	Fundy, NS	4	1	Low	Data quality good

3. Shoreline Extraction : Polarimetric analysis

A method was developed so that from any image data (either contrast enhanced or single channel) a waterline estimate could be extracted.

Two categories of analysis were developed here: (1) polarimetric methods were implemented to enhance the contrast between the land and ocean (Section 3.2.2) and to extract shore slope information (Section 3.2.1) and (2) a methodology, involving several analysis tools (which were independent of the data type) was developed for extracting the shoreline from an enhanced image (Section 3.3). For this first category the objectives are: (a) evaluate several polarimetric contrast methods for extracting features such as the waterline, (b) determine if other information, such as surface velocity, can be used to improve estimates, and (c) implement polarimetric data segmentors or classifiers for feature attribute applications.

This section is organized as follows. First geometrical and calibration processing is described. This is followed by a description of the polarimetric methods used for extracting shore slope information and for enhancing the contrast between land and water. Finally the shoreline extraction procedure is described.

3.1 Imagery post-processing : geometric and calibration

During the time of analysis, no geocoded product was available for the complex data type used in this study. Consequently, Ground Control Points (GCPs) and interpolation were used for geo-referencing the shoreline vectors. Since all of the environments were fairly flat this approach will not introduce any significant error. The positional errors for all of the waterline data shown here is between 6.5 and 7.5 m (4 m wave variation, 1 m GPS error, 5 m GCP pixel size error). Sufficient GCPs were difficult to obtain for some of the more rural scenes. Fortunately the environments studied here were relatively flat; thereby reducing errors incurred by fitting geographic co-ordinates based on GCPs. This error would likely be comparable to the RADARSAT 2 fine beam polarimetric image if GCPs are used for geo-referencing purposes. Alternatively, if RADARSAT 2's position is well known, as expected, then the image positions can be geocoded with small error estimates. The positions can also be improved if DEMs (Digital Elevation Maps) are available.

3.2 Polarimetric exploitation methods

Two types of analysis methods studied for this project are presented in the following subsections; 1) shoreline slope extraction and 2) polarimetric contrast enhancement techniques.

3.2.1 Shoreline Slope Extraction Method

The intention of this study was to extract a shoreline from only one image scene using polarimetric methods and to explore methods such as shoreline slope extraction which would

improve the estimate to a vector referenced to the tides (e.g. MHWL). Other studies [2-5] have used several images to deduce a shoreline slope from the extracted waterlines which are linked to tidal elevations. If by any method the shore slope is extracted, then with sufficient tidal elevation information [8, 9], a MHWL can be estimated by projecting to the shore slope the difference between the MHWL elevation and an *in situ* tidal elevation. This project investigated one polarimetric method to extract shore slopes using only one image scene.

There are many imagery methods which can be used to determine shoreline slopes. One method utilizes spatial wave-number information determined from the backscattered signatures of the ocean surface to estimate the bathymetry. This method has had some success for north European shores [30, 31, 32] but still require further research. Another method has had some success predicting land topographic slopes, with errors of about 1°, using polarimetric imagery. This method measures the target tilt perpendicular to the SAR's LOS. Offsets from a 'model' polarization response (see Section 3.2.2) determines a target's orientation [33, 34, 35] perpendicular to the LOS. This method was studied here. Since the offset measured is not the true topographical slope, some knowledge of the topography in the slant range direction is required (if DEMs are available). Alternatively, if the SAR path is perpendicular to the shoreline then this offset would be near the true slope for most shorelines. For all experiment sites, at least one SAR line was flown nearly perpendicular to the shoreline.

An optimal time to extract shoreline slopes would be at low tide when the entire foreshore area is exposed. Data were collected from both sites for this application. The Bay of Fundy is an ideal shore to test the slope extraction method but this data was not available. Fortunately we acquired imagery collected a year after the Fundy experiment in the same region (line 4 pass 1, Nov 10, 1999). We investigated these data to determine if shore slopes could be obtained. The analysis was tested on imagery collected during low tide over a large mud flat region where the slope is nearly zero. Extraction of the shoreline slope was also attempted with Duck, NC imagery and compared to topographic and bathymetric measurements of the shore site acquired about one month before and after the experiment [e.g. data on the Field Research Facility (FRF) web site: www.frf.usace.army.mil].

3.2.2 Polarimetric Discriminators

Several polarimetric methods were investigated here for the purposes of enhancing the contrast and detecting either the debris line, vegetated shoreline or the *in situ* waterline. Depending on the phenomenological characteristics, either one or all of these vector lines are usually detectable from one of the several different types of polarimetric applications used in this study.

The contrast between land and ocean in SAR imagery is usually large. For this reason very simple approaches (e.g. single channel, span) were taken. However, for regions with large energetic waves, such as at Duck, NC, more selective methods were required. All methods used for this study are described briefly below.

(1) The logarithm of the span was one method used here for extracting a waterline. The span effectively represents the total power of the scattering matrix and emphasizes the water line edge because the backscatter magnitude decreases steeply between land and water.

(2)The logarithm of the Pre-Whitening Filter (PWF) [36] was also used since it also represents power after filtered for speckle noise. These two methods (span and PWF) were appropriate for shorelines where the backscattering contrast between the ocean and land was large. The logarithm of these two parameters was implemented to reduce small scale variability.

(3) Another method tried here was to determine optimal polarization response filters [37, 38, 39]. The polarization response is a method which provides information about the scatterer. It uses the scattering matrix information to calculate M, the Stokes scattering matrix,

$$M = \tilde{R}^{-1}WR^{-1},$$

$$W = \begin{bmatrix} S_{vv}^* S_{vv} & S_{vh}^* S_{vh} & S_{vh}^* S_{vv} & S_{vv}^* S_{vh} \\ S_{hv}^* S_{hv} & S_{hh}^* S_{hh} & S_{hh}^* S_{hv} & S_{hv}^* S_{hh} \\ S_{hv}^* S_{vv} & S_{hh}^* S_{vh} & S_{hh}^* S_{vv} & S_{hv}^* S_{vh} \\ S_{vv}^* S_{hv} & S_{vh}^* S_{hh} & S_{vh}^* S_{hv} & S_{vv}^* S_{hh} \end{bmatrix},$$

$$R = \begin{bmatrix} 1 & 1 & 0 & 0 \\ 1 & -1 & 0 & 0 \\ 0 & 0 & 1 & 1 \\ 0 & 0 & -i & i \end{bmatrix},$$

where $i = \sqrt{-1}$, $\sim$ represents the transpose, and $*$ represents the complex conjugate. From this matrix the backscattering coefficient, ξ, from any transmitted and scattered orientation, ψ, and ellipticity, χ, angles can be calculated by

$$\xi(\psi^{sc}, \chi^{sc}, \psi^{tr}, \chi^{tr}) = A^{sc} \cdot \langle M \rangle A^{tr},$$

where,

$$A = Rg,$$

and

$$g = \begin{bmatrix} p_v p_v^* \\ p_h p_h^* \\ p_v p_h^* \\ p_h p_v^* \end{bmatrix}.$$

Here

$$p^\eta = \frac{E^\eta}{|E^\eta|}, \eta = sc, tr$$

and E and $\langle \ \rangle$ represent respectively the electric field vector and the expectation operator.

For a polarization response filter, ξ, there are transmit and receive ellipticity (χ) and orientation (ψ) angles which are optimal for enhancing the contrast between two types of clutter. For this experiment, optimal responses were chosen to differentiate between ocean and land based on the co-polarized and cross-polarized responses only. For the Bay of Fundy,

which is a more natural environment, the optimal response was very near the HH component, while for the Duck region, a semi-urban environment, the optimal response was variable. For urban areas it was found that optimal responses were very near the results of Swartz et al [39]. In order to retain the sharpness of the waterline interface, but reduce speckle from the Single Look Complex (SLC) images, a summation

$$\Psi = \sum_J \xi(\psi^{sc}{}_j, \chi^{sc}{}_j, \psi^{tr}{}_j, \chi^{tr}{}_j)$$

of several of these filters at or near (within fifteen degrees) an optimal response filter was used. Alternatively, a summation over rural and urban filters was used for a mixed urban and natural environment.

(4) The complex correlation coefficient, ρ, between the HV and VH channels was also used as an indicator for the shoreline. These channels were compared for three reasons: 1) the dynamic range between land and water is large, 2) ocean wave structures are well defined in the cross-channel imagery and 3) the phase differences between the two channels are indicative of either motion or changing clutter and these effectively weight the correlation function such that its magnitude reduces with phase difference. The cross-polarization correlation coefficient,

$$\rho = \frac{\left\langle S_{HV} \cdot S_{VH}{}^* \right\rangle}{\left\langle \sqrt{|S_{HV}|^2} \right\rangle \left\langle \sqrt{|S_{VH}|^2} \right\rangle}$$

was estimated by the spatial sample average over at most 3 range and 3 azimuth pixels. The number of averages was limited in order to reduce the degradation of the shoreline edge.

(5) Another measure of coherence was also used and is referred to here as the weighted cross-polarization coherence,

$$\rho_w = \Re \left\{ \frac{S_{HV} \cdot S_{VH}{}^*}{\sqrt{|S_{HV}|^2 |S_{VH}|^2}} \right\} W,$$

$$\rho_w = A_{HV} A_{VH} \cos(\varphi_{HV} - \varphi_{VH})$$

where $A_{HV}, A_{VH}, \phi_{HV}, \phi_{VH}, \Re$ and W refer respectively to the HV and VH channel amplitudes and phases, the real part of a complex number and a weight factor. The weight factor implemented was the denominator, $\sqrt{|S_{HV}|^2 |S_{VH}|^2}$ which was chosen because it preferentially weighted land backscatter values. The real component of the coherence is effectively weighted by the phase difference, thereby reducing the magnitude for regions of motion or topographic change.

(6) An exponential weight was also used with any of the above discrimination methods. This weight is based on the phase difference between the HV and VH channels. In particular, the cross-polarization phase difference,

$$\phi = \tan^{-1} \left(\frac{\Im(S_{HV} \cdot S_{VH}{}^*)}{\Re(S_{HV} \cdot S_{VH}{}^*)} \right)$$

was implemented for identifying regions of motion or target type change, where $\Im$ represents the imaginary part of a complex number. This was particularly useful for regions where there was significant motion due to large tidal waves. In these regions, it was particularly difficult to distinguish land from water since the backscatter values from the breaking waves were comparable to the land. Figure 10a shows how well the PWF discriminates the land in a Duck scene, while in Figure 10b the phase difference, $|\phi|$ emphasizes areas where motion or topographic change occurs. For the ocean environment this phase difference is almost entirely due to motion while for the steep beach area it is likely due to topographic change. This phase difference was used as a weight,

$$\lambda = e^{-|\phi/\pi|}$$

for many of the other discriminators so that regions of motion (like the ocean) would be weighted less than stationary regions (like land). This weight was particularly useful for the Duck region where the land-water definition is poor.

(7) Single-channel imagery of the HH and HV components were also used for estimating the shoreline vectors in order to compare single channel and polarimetric methods. HH was an optimal channel for rural, Nova Scotian sites (as discovered with the optimal polarimetric response study) and ocean wave structures are often captured in HV channel data.

(8) Also examined were classification methods described by for instance Cloude, Pottier and Lee [17, 18, 19] using a coherency matrix,

$$\langle |T| \rangle = \frac{1}{N} \sum_{j=1}^{N} k_j \cdot k_j^T ,$$

where N, is the number of pixel averages, superscript T represents the complex conjugate transpose, and,

$$k = \frac{1}{\sqrt{2}} \begin{bmatrix} S_{HH} + S_{VV} \\ S_{HH} - S_{VV} \\ 2S_{HV} \end{bmatrix} .$$

From the coherency matrix, eigenvalues can be calculated to determine a measure of the entropy, H, and, from parameterization of the eigenvectors, α, a measure of the scattering mechanism, can be calculated. Classification zones are then defined on the H-α plane and the distance from the zone centres are delimited by the complex Wishart distribution [17, 18, 19] which represents the distribution of the averaged coherency matrix. This method was used here for extracting the shoreline and for feature classification. It has the potential of identifying the beach area so that other areas can be masked out, thereby reducing the computational effort.

3.3 Shoreline extraction

The shoreline extraction procedure consisted of the following steps: 1) the data (any image data with or without contrast enhancement by any method in §3.2) were filtered to remove any speckle effects (if appropriate for the data type), 2) the imagery were interpolated or sub-sampled for better resolution, 3) shoreline edges were extracted based on clutter statistics, and

4) the extraneous vector lines are removed through a sieve method. Each of these steps are discussed further below. In Figure11, this procedure is shown in flow chart form.

Each of these processes were made as automatic as possible with some supervision. However, for some shore regions the land and water backscatter magnitudes were comparable and more supervision was required.

Filters were chosen to reduce the speckle but with minimal edge degradation. Filters included the median [40], and Lee [41]. The Lee filter was applied after interpolation so that the pixel dimensions were square.

Interpolation (i.e. using Fourier methods) in the range dimension was used to improve the estimate since the land-water interface was, in a sense, a boundary between two continua. One problem associated with interpolation (interpolation in the spatial frequency domain) is spectral leakage, particularly in a coastal environment where the dynamic range is large between land and water. In order to reduce this problem, despiking was implemented for large image spikes (on land), since this lost information is not pertinent for this application. In general, this interpolation resulted in smoother and often more accurate shoreline vectors, provided large spikes on land were removed.

Several edge detectors were investigated [40], but none of them produced a shoreline vector which was easily extractable. For this project, contour algorithms were used to extract shorelines at prescribed thresholds. Thresholds were determined by three different methods : (a) detecting the minimum point between a bimodal distribution (i.e. land and water clutter distributions), (b) calculating the midpoint between land and water mean values and (c) thresholds $X=\mu+t\sigma$ where μ and σ are the ocean clutter mean and standard deviation and t is some constant (for this study, t=1,2). The results from all these methods did not produce significantly different shorelines, primarily because for most environments there is a sharp boundary between the land and water interface in the imagery. Duck, NC was the exception since the contrast between the beach and intermittent breaking waves was small.

When the contour algorithms were applied to the data at a given threshold limit, edges for other bodies of water (e.g. lakes) were also extracted in a scene. For simpler environments, such as the Bay of Fundy, it was easy to discard these extraneous shorelines on land with image morphological techniques such as sieve methods, which remove closed contours and short vector lines. However, for areas like the Duck Shoreline, it was much more difficult to extract the waterline (although the extraction of the vegetation line was easily accomplished with minimal supervision) in an unsupervised fashion since there were regions in the image where the land and water backscatter values were comparable. The water line was visually apparent in these more complex images, but the threshold method selected erratic shorelines in some places due to the intermittent bright waves against the dark beach in the image scenes. For these cases, the waterline extraction required extra attention. This was achieved by masking out (or clipping) regions, in a supervised fashion, where the extracted shorelines were confused due to poor distinction between land and water. The resultant data gaps were connected by linear interpolation.
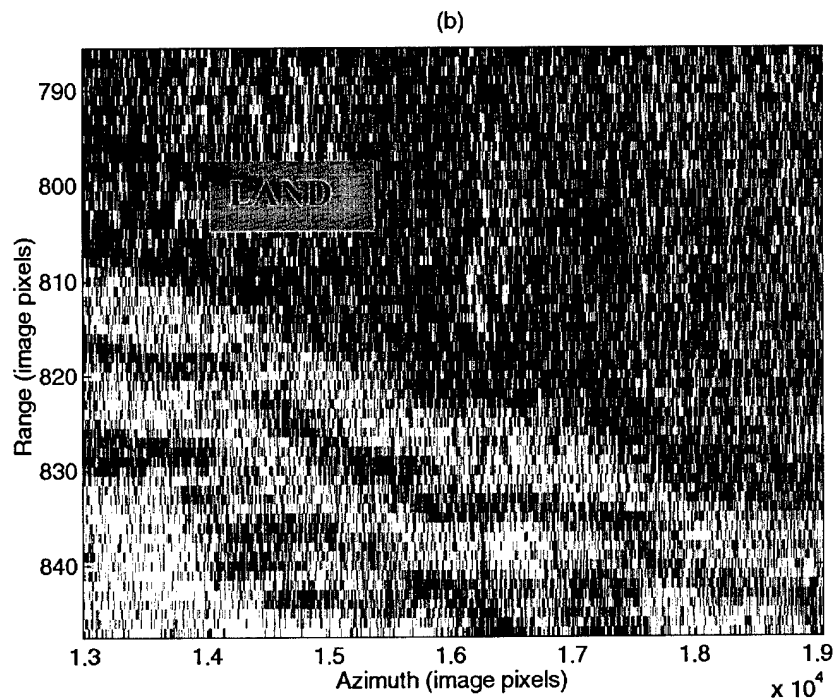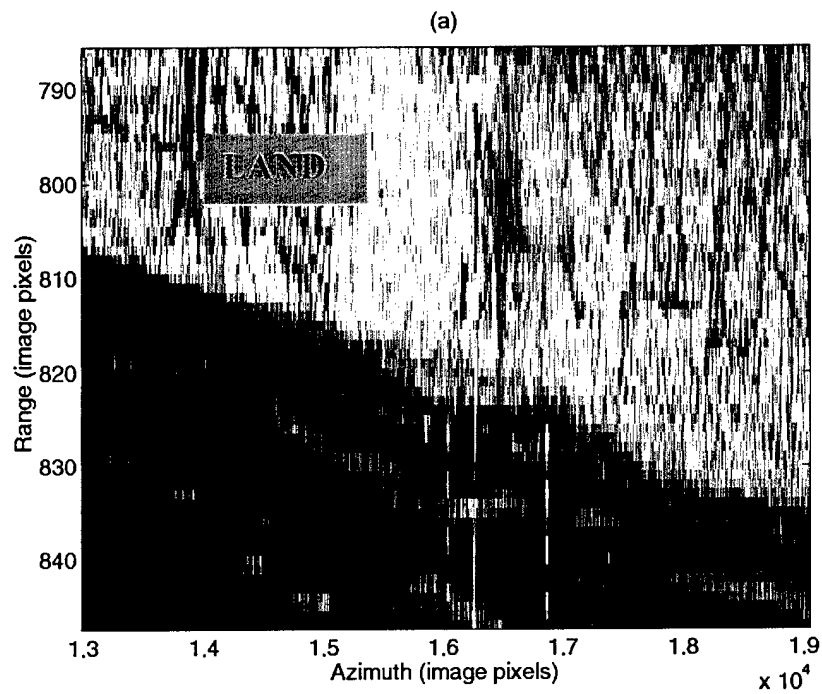
Figure 10. Land and water detection. Analysis of Duck, NC scene, line 6 pass 1, emphasizing stationary and non-stationary surfaces where a) is the PWF which detects stationary land surfaces, while b) is |φ|, the absolute value of the phase difference between the cross polarized channels, which accentuates non-stationary regions of motion (e.g. ocean) or target change. The axes are in image pixel co-ordinates and range and azimuth lengths are 350 m and 2.4 km.
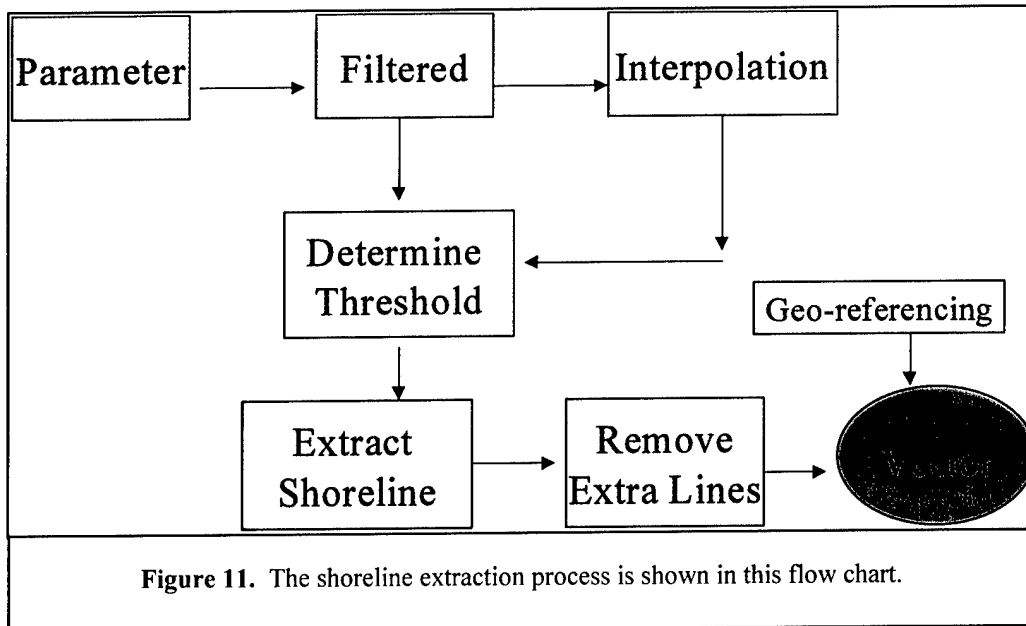
Figure 11. The shoreline extraction process is shown in this flow chart.

4. Results

4.1 Visual and quantitative analysis

Several SAR scenes from the two regions, North Carolina and Nova Scotia, were studied here using methods documented in Section 3. Reasonable shorelines were extracted from all the images although the images at Duck, NC, were particularly difficult to analyze because there was very little contrast in the image signature at the land-water boundary. Below, a brief overview of the results is followed by more detailed discussions for each site. General discussions and recommendations are found at the end of this section.

In this study, for locations where the image contrast between land and water is well defined (e.g. Nova Scotia), the debris or waterline extraction did not require very sophisticated methods. Single-channel data such as the HH or HV component produced reasonable results since the difference between the ocean and land clutter was large. Other contrast enhanced data types (such as the span or the PWF) reduced speckle noise and produced slightly better results. For imagery with well defined shoreline signatures (such as images of the Fundy beach environment), the waterline extraction was relatively automatic and required minimal supervision. In contrast, for regions (e.g. Duck, NC) where the image contrast between land and water signatures was small and intermittent, the parameter used for the waterline extraction became more relevant and the process required more supervision. It should be noted however, that while it was difficult to extract waterlines at Duck, it was very easy to extract semi-automatically the vegetation line. Depending on the mapping accuracy required, the vegetation line may be sufficient as a waterline estimate. For the Duck shoreline, the vegetation line provided estimates which were typically 30 m from the waterline.

Phenomenological differences between the two regions contributed to the decision process or logic used to extract waterlines. This logic was based on evidence from ground truthing. Without these ground truthing results, incorrect image interpretations and extracted shorelines would have been the result. For instance, as demonstrated in Figures 5 and 8 and § 2.1.1, image phenomenology can be related to different beach characteristics which correspond with the local wave dynamics.

For instance, the Bay of Fundy (Figure 5) with gentle wave features has fine clay to sand to gravel transitions from the foreshore to high tide waterline. For images acquired at high tide, this results in a large backscatter difference between the larger beach particles (e.g gravel) and the relatively smooth ocean surface (provided the ocean surface is not very rough). For images acquired at low tide the backscatter contrast from the land-water boundary is small but often distinguishable. The small backscatter from the foreshore region at low tide is due to specular reflection because at Fundy, these regions are very smooth.

For more dynamical tidal regions, such as at Duck, NC, the beach sand is coarse and well drained which results in very little backscatter (and which appears in a SAR image like Figure 8, as a dark signature. The beach signature (dark) in the imagery is sandwiched between two large backscatter regions (i.e. bright image contrast regions at the breaking wave and vegetated land interfaces, as shown in Figure 8). Hence, in these images there are at least two

edges with large contrast that potentially could be the waterline. A decision process or logic is required in order to select the edge which defines the best waterline. This is more difficult compared to the Fundy shoreline where only one edge near the waterline was evident in the imagery and the beach was bright and not dark. However, if one is aware of these types of image phenomena, which are related to the dynamics of the tidal waves and associated sedimentology, a logical process can be used to select the best waterline. For sand beach environments where large waves occur, the first wave structure next to the "dark" beach signature is selected as the waterline and is distinguished from the extraction of the vegetation line. For data where the image signature indicated that the ocean wave structures were significant, and where there were two distinct contrast edges, this logic was applied. For instance, using this logic resulted in extracted shorelines very near the measured waterline for both Camp Lejeune and Duck data. The same phenomenology is relevant for these two locations which are separated by a distance of 300 km.
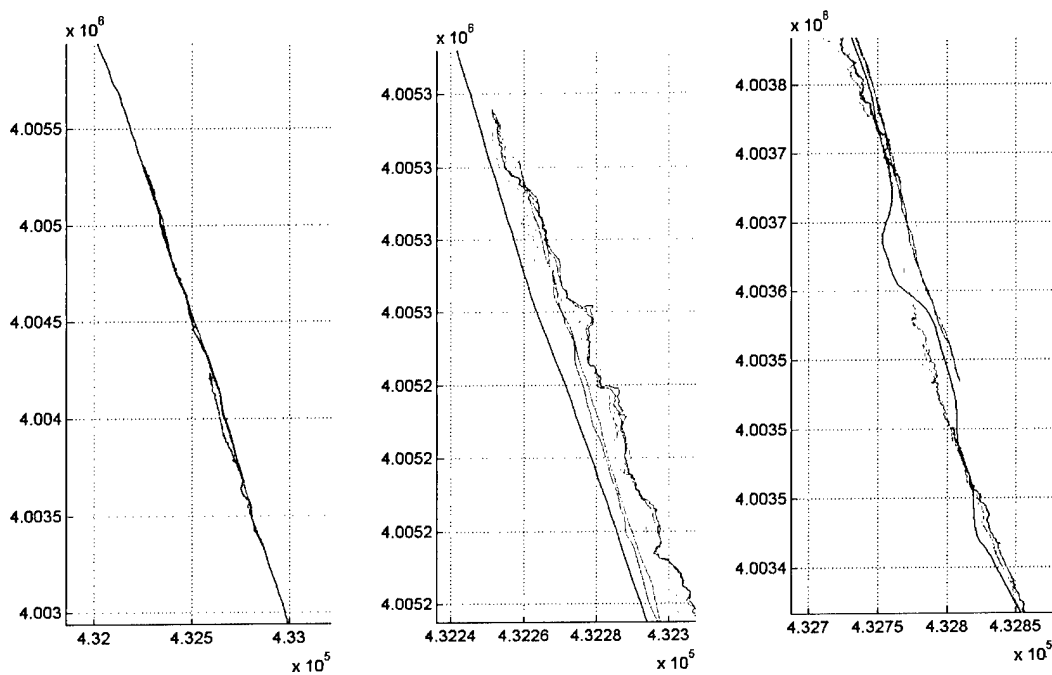
Figure 12. Comparison between Duck (line 6, pass 1, low tide) measured and extracted shorelines from imagery. The plot on the left compares the Mean High Water Line (MHWL) surveyed estimate with shorelines extracted by different analysis methods. The two adjacent plots are close-ups of this left most plot. Here the solid black line is the surveyed MHWL estimate, the mauve line is the *in situ* measured line (two waterlines from a GPS survey back and forth along the beach), the red, green, blue and cyan lines represent extracted shorelines from different discrimination methods implemented and are discussed further in the text (§ 4.1). The axes are in Northing (ordinate) and Easting (abscissa) coordinates (NAD83).

In general, many of the contrast enhancement methods produced similar shoreline results although some were slightly better than others. Some extracted waterlines are compared in Figure 12 (Duck line 6, pass 1 acquired at low tide) with GPS data collected at the waterline during the SAR acquisition. These results are typical for most sites. Here the black line is the

26

MHWL surveyed estimate and the mauve line is the *in situ* GPS waterline measurement which was recorded along the beach in both directions (back and forth) in order to demonstrate the tidal level change over about a one hour time period. The [red, green, blue, cyan] lines are extracted shorelines [for respectively: log(PWF), weighted cross-polarization coherence with exponential weight, λ, PWF with exponential weight, λ, and PWF with exponential weight, λ, and range interpolation]. As can be seen in the image all these waterline estimates are similar. The range interpolated extracted shorelines were often slightly better estimates that produced smoother lines. PWF and weighted coherence, ρ_W, produced slightly better estimates than other methods such as single channel, span, optimal responses and the cross-polarized correlation, ρ. Also, for environments with large wave action (i.e. NC), the exponential weight, λ, improved the results for all methods.

Error estimates between measured shorelines and extracted shorelines (from imagery) were compared using two methods. One method, proposed by NIMA [10], was used here to calculate an estimate for one extracted shoreline (see § 4.1.2). Another method was implemented here to produce error estimates for all the shorelines analyzed in this report. This method integrated the area between two shorelines (estimated and reference shoreline vectors), normalized by the length of the reference shoreline (either ground truthed waterline or MHWL). These vector shorelines were based on a polynomial fit to the shoreline data (ground truthed and detected). This was required because there were data gaps in both the measured and extracted shorelines. Error estimates between the measured and reference shorelines (i.e. either the waterline [wl] at image time or the MHWL [Duck only]) are presented in Table 2. As can be seen in the results, these mean error estimates ranged between 0.2 and 10.4 m. Both error estimate methods (NIMA's and the method used in this report) produced similar results (i.e. respectively 6.3 and 6.8 m error when compared to the MHWL for the Duck line 6, pass 1, low tide image).

Table 2. Error estimates between the extracted shoreline and either the ground truthed waterlines (wl) or the measured MHWL at Duck, NC.

Date	Site	Line #	Pass #	Tidal Stage	Length (km)	Error- wl (m)	Error- MHWL (m)
11/23/98	Fundy	2	1	High	1.3	3.8	N/A
10/3/99	Duck	6	1	Low	2.0	10.4	6.8
10/3/99	Duck	7	2	High	1.5	1.7	6.3
10/3/99	Duck	7	2	Low	1.7	4.4	8.4
10/3/99	Duck	8	3	High	2.0	5.9	7.8
10/4/99	Lejeune	1	1	Low	3.6	0.2	N/A
10/4/99	Lejeune	2	2	Low	2.6	8.6	N/A

There was significant spectral leakage from the land into the water for many of the image data sets (see Figure 13). In particular, this problem was quite significant in the Duck imagery which is a low density urban environment. It is likely that these attributes are due to the airborne SAR's data acquisition system which records data in a range compressed form, thereby reducing the dynamic range capability. This can result in data with saturated or underflow characteristics and may account for the streaks observed in the imagery from the land into the ocean. The motion of the tidal wave structures may also contribute or have an

effect on these streaks. In particular, at Duck, significant longshore currents occur and edge waves erode the shoreline so that scalloped beaches known as cusps are formed. Associated with the cusps and edge waves are also rip tides. It is likely that many of these oceanographic features contributed artefacts to the SAR image such as, azimuthal smearing and wave bunching effects [29]. However, these wave velocities (edge and longshore) are usually parallel to the shore and vary in speed as a function of cross-shore direction, with very localized regions of high velocity (1-2 m/s) at regions of decreasing water depth (i.e. near the shore and submarine sand dunes) and small velocities elsewhere (0.4 m/s). These higher wave velocities can cause significant SAR image azimuthal offsets for cases when SAR flights are perpendicular to the wave direction. In Figure 13, these wave types (edge, longshore) are almost perpendicular to the SAR, which would be the optimal condition for azimuthal image effects. Since the larger velocities are localized, it would seem likely that the streaks, observed in Figure 13, would have more variability along the streak, which does not seem to be the case here.

SAR images of environments like Duck, where large tidal waves occur, generally have image effects from the wave motion, particularly when the SAR path is perpendicular to this motion. However, it is not certain what proportion of the streaking (for instance, in Figure 13) is due to this wave motion or due to saturation effects from the SAR system. This streaking effect was not observed in the single channel RADARSAT and ERS data, but was observed, although to a lesser degree in the polarimetric SAR Fundy data where the wave motion is relatively smaller. In addition, several saturated regions in the signal data were found to be associated with many of the image streaks, for the Duck, line 8, pass 3 data. These facts are indicative that the streaking observed in the imagery is largely due to the saturation effects from this particular SAR system. The other three images studied at Duck were flown parallel to the beach instead and would be influenced more by incoming breaking waves. Spectral leakage effects were more dominant for the scenes where the ocean was at near range (e.g. Duck line 8, pass 3). This is the most difficult condition to acquire proper gain settings for the SAR system used in this experiment. This effect is not expected to be as significant a problem for RADARSAT 2 data, except that attention will be required for selecting the correct gain setting.

The beach signatures in the North Carolina imagery had less contrast at the land-water interface than at Fundy. For the NC regions, applying the exponential weight (i.e. HV-VH phase difference) to any of the methods in Section 3 improved the results and reduced the supervision required for extracting the waterline. It was difficult to extract the waterlines because their signature in the imagery was indistinct and intermittent, which may be an artefact of ocean related effects such as wave bunching [29]. For these difficult regions, we corrected these problems by manually cropping the regions where the extracted shoreline process became confused due to this intermittent characteristic. For the Duck data, this waterline was usually detectable by the human eye, but it was quite difficult to automatically extract it from imagery. Because of the supervised cropping there were data gaps in the extracted shoreline. For the Duck data, the use of the coherence between the cross polarization channels HV and VH improved the results. It is possible, however, that Radarsat 2 which will have poorer resolution and less power, may not be able to utilise this information.

Topographic slope extractions for the beach areas were studied here in order to determine if MHWL estimates could be calculated from waterline vectors. Image lines at both regions were flown nearly perpendicular to the shore within about 15°. The results are not conclusive and are explained further for each site.
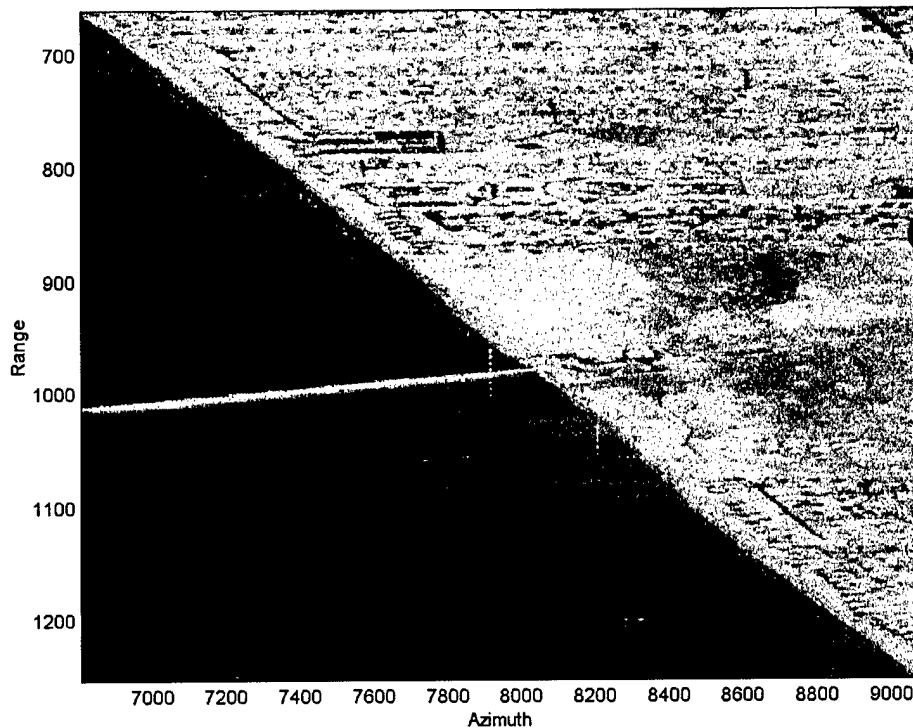
Figure 13. An image of Duck (line 8 pass 3, low tide), which demonstrates the streaks (documented in § 4.1) extending from the land into the ocean. These streaks increased the difficulty of extracting shorelines from imagery. This image is about 3 km x 850 m in range and azimuth.

4.1.1 Bay of Fundy

The Bay of Fundy (image data shown in Fig. 5) is a rural area. The image contrast between land and ocean was large. Methods such as a single-channel, span, PWF or weighted coherence methods produced reasonable contrast for extracting shorelines with minimal supervision.

A shoreline extracted from a Bay of Fundy image that was acquired at high tide, is shown in Figure 14. This waterline was extracted from the logarithm of the HH component (power) to demonstrate that single channel results are reasonable for shorelines like the Fundy coastline. The ground truthed vector shoreline measured by GPS from the helicopter is also shown and it indicates that the average (maximum) difference between the extracted waterline and *in situ* GPS measurement is about 7 m (30 m) horizontally, which is near the experimental uncertainty of ±7.5 m. The GPS measurements were taken from a helicopter which did not

capture some of the more smaller features, such as streams. The extraction method detected an inlet near 5017350 Northing (NAD83). Also at 5017750 Northing is a pebble-mud interface region where it is speculated that there is some drainage from the marsh which is directly next to the beach area.

Since the Fundy low tide data was not recoverable from the recording media, we analysed another low tide data set from the same area which was collected the following year (Nov 10, 1999). The image analysed was a tidal flat area where the slopes are near zero. Our resultant shoreline slope estimate for this tidal flat was about zero and the quality of the responses used for this estimate looked good, unlike the responses from Duck's beaches. No ground truthing is available for this analysed area at the present time. However the analysis results indicate that this method potentially could be useful for extracting shoreline slopes. Further well ground truthed studies are required to validate this.
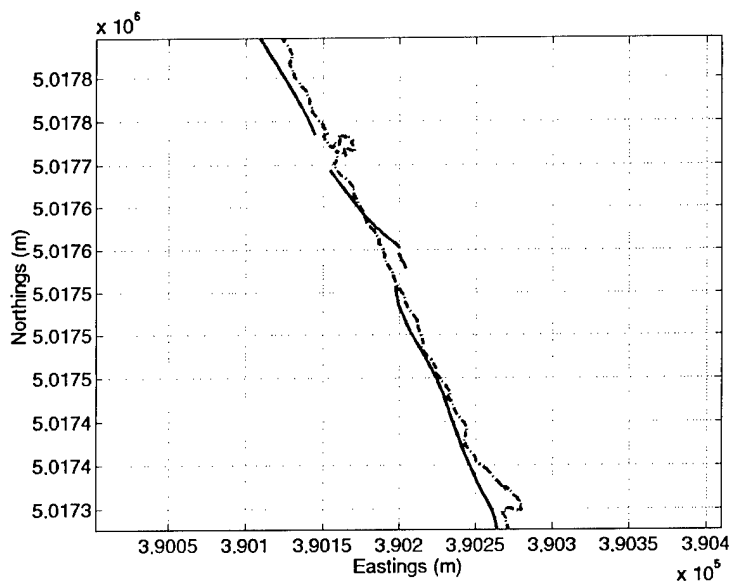
Figure 14. The dotted line represents the extracted waterline at the Bay of Fundy (image data shown in Fig. 5) from the logarithm of the HH power. The solid line is the GPS *in situ* measured waterline from the helicopter platform. The gridlines are every 50 m and the axes are in NAD83 co-ordinates. Stream locations are discussed in Section 4.1.1.

4.1.2 Duck, North Carolina

Four Duck images were processed for analysis. Most of these Duck images had several attributes which made the data difficult to analyze. These included spectral leakage problems and an unexplained signal in the system's byte noise data (line 7 pass 2 high tide and line 8 pass 3 high tide images). This noise data is implemented for radiometric calibration but can be replaced with thermal noise values instead with some loss of the absolute radiometry. The spectral leakage problems (Figure 13) are due, dominantly, to the limitations of the airborne acquisition system and not due to polarimetric SAR. Therefore this artefact is not expected with the RADARSAT 2 data. The unexplained signal in the noise data may be related to

other experiments in the area or a SAR system problem. Since this noise problem has not been observed in other data, it is speculated that other systems may have interfered.

Extracting shorelines from the vegetation line signature in the Duck image data was relatively simple and automatic. In contrast the extraction of the waterline from the same data required significant supervision and effort, with the exception of the line 6, pass 1, low tide scene, which had the best image quality from the Duck data set (Figure 15). The increased difficulty of waterline extraction at Duck, is likely related to the spectral leakage problems in these data, and also to SAR image effects from the tidal wave motion during the image acquisition. Since the land-water contrast for these imaged NC beaches is small, these effects have a greater impact. For this SAR, it is easier to avoid these saturation and spectral leakage effects when land and not a water body is in the near swath. This may explain why the waterline extraction was much easier and the image streak effect were less for image data acquired with land in the near swath (such as line 6, pass 1, low tide data) than for other image scenes (such as line 7, pass 2, high and low tide, and line 8, pass 3 high tide), which were imaged with the ocean in the near swath. The line 8 pass 3 high tide data (Figure 13) was the only Duck scene available for determining shore slope information. Unfortunately, the streaking in this image was significant, reducing the confidence and quality of these results. It is speculated that the streaking was predominantly due to spectral leakage, but that SAR image effects from ocean motion, and large scattering surfaces from oceanographic processes (e.g. rip tides, breaking waves, as discussed in § 4.1) also contributed.

Waterlines were extracted from all available scenes with data gaps in these shorelines which were related to data quality problems such as spectral leakage from the land into the water (in Figure 13). In Figure 16, a comparison of the measured MHWL with a portion of the extracted waterline indicates that the difference can be as much as 30 m. A method which is described in [10] was used to compute the error from an extracted waterline (line 6 pass 1) with the surveyed MHWL. The average error was found to be 6.3 m over a distance of 2 km. The error estimate method used in this report (see Table 2) for this same waterline is 6.8 m.

Beaches are relatively smooth surfaces, so it seemed possible that the shore slopes could be extracted from polarimetric images. The Duck beach surface was relatively smooth in some areas. However, there were several areas where the beach area was quite rough since any physical disturbance in this coarse sand persisted, provided ocean waves did not flow over the surface. The shore slope analysis from this data set was not successful and did not produce reasonable or consistent shoreline slopes. The quality of the responses used for the analysis were poor and seemed to be affected by more than one scatter type. Spectral leakage problems from the land into the ocean may be one reason. Additional factors are: (1) the shoreline width was small in pixel dimensions, (2) two distinct boundaries on either side of the beach, and (3) SAR image effects from the large waves nearby.

The Cloude coherence method [17] using the Wishart distribution (Figure 17) segments different environment classes in the littoral region quite well. For this example the image data was classified into nine zones. Note in Figure 17 that the beach is well defined as a zone. Here the *in situ* GPS waterline vector and sand dune / vegetation line delimit the beach zone
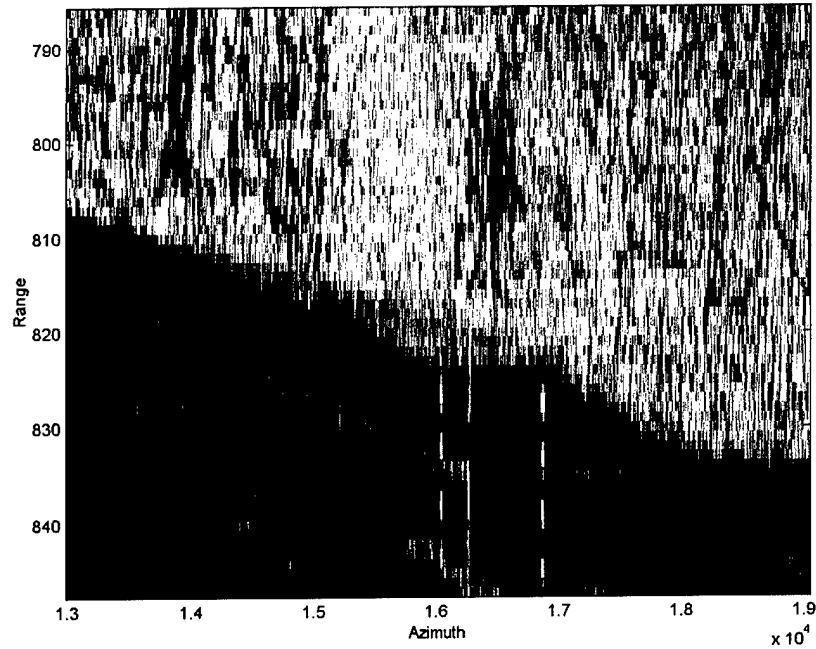
Figure 15. Duck, North Carolina coast. The green line is the *in situ* measured waterline (GPS) and the red line is the waterline extracted from the imagery. The axes are in image coordinates with range and azimuth lengths about 350 m and 2.4 km. Note that a pier extends into the water near the 16300 azimuthal line. On either side of it are dashed lines which represents the effect from Active Radar Calibrators (ARCs). The Red, green and blue image composite represents HH, HV and VV.
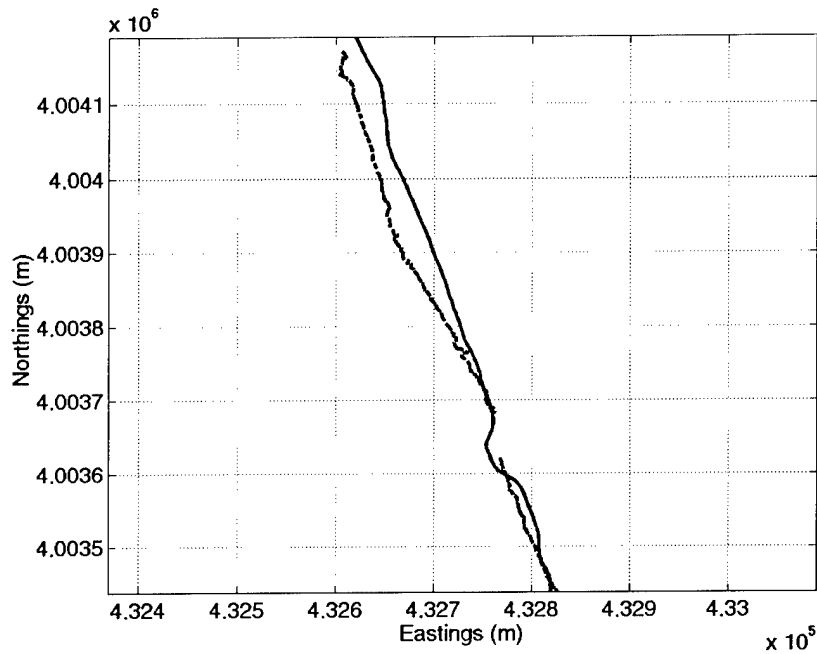
Figure 16. The extracted shoreline vector (dotted) is compared with the measured MHWL (solid) for a Duck, NC image (line 6, pass 1). Axes are in NAD-83 co-ordinates and grid lines are 100 m apart.

on either side. Because pixel averaging is a basic part of this procedure, the waterline edge may not be as precise (the error between measured and the extracted shoreline was found to be about 20 m for this image). However for most required mapping accuracies, this incurred error is tolerable. For these data, this method provides reasonable shorelines, although the error was often larger than other methods studied here. This method could also be used for masking areas outside the region of interest, thereby reducing computational efforts. Classifying methods, like the Cloude method, have the potential to provide attribute information which would be beneficial for classification of the imaged environment. An internal DREO report in progress [43] discusses classification capabilities in the beach area using this method.
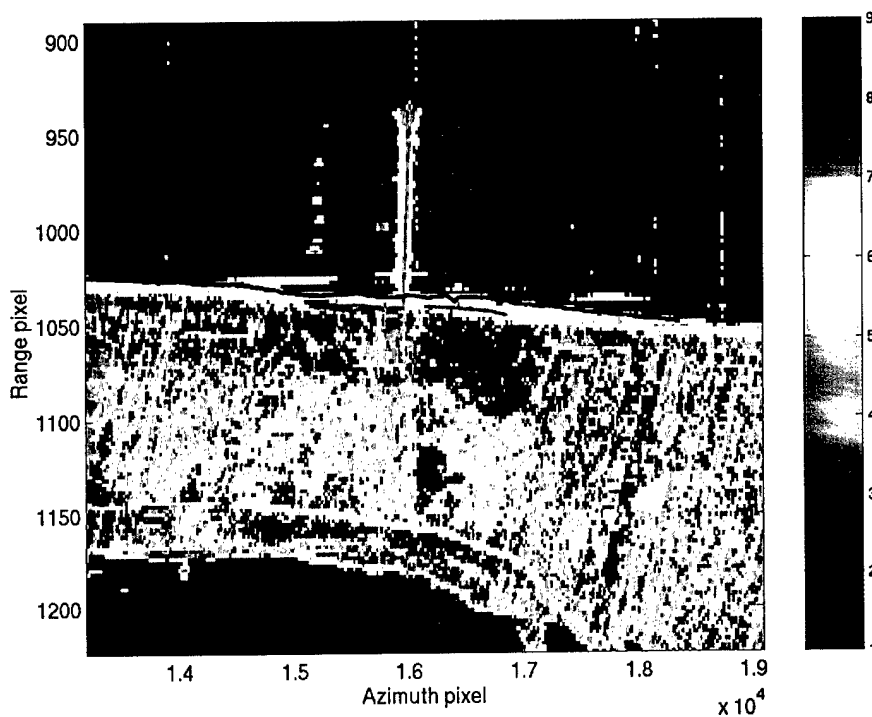
Figure 17. Coherence method using the Wishart distribution discriminates clutter into 9 zones. Here it segments the beach area into one zone. The black line represents the *in situ* GPS measured waterline and the red lines indicate the top and bottom of the sand dune cliff where the vegetation on land begins. The axes are in image pixel coordinates. The range and azimuth lengths are about 1.7 km and 2.4 km. Note the pier and buoy array (to the left of the pier).

4.1.3 Camp Lejeune

Two low tide Camp Lejeune scenes were analyzed: line 1 pass 1 and line 2 pass 2. The Camp LeJeune's image quality, in general, was superior to the Duck image quality. This may be due to one or a combination of the following reasons. This region was not as urbanized and therefore saturation at the shoreline resulting in spectral leakage occurred less. The waves were slightly less dynamic, and the images' waterline signature was more distinct than in the

Duck images. Consequently, the Camp Lejeune shoreline extraction required very little supervision relative to the Duck analysis.

The extracted shoreline results are very near the *in situ* waterline as shown in Figures 18 and 19 with average errors <10 m and maximum errors of about 30 m when compared to *in situ* GPS measurements. The maximum errors occurred at a region where the beach slope became more shallow and the beach widened to a flatter, smooth surface with finer sand particles. This is an area where the waterline is most variable because it is a very flat region. Note that a significant portion of the extracted LIDAR waterline is at least 50 m from the *in situ* GPS waterline. Although the LIDAR measurements were taken a few weeks after the experiment, it is unlikely that these differences would be so large, based on the beach dimensions. These comparisons will be discussed further in [10].

4.2 Interpretation and discussion

Shorelines were successfully extracted for all three sites (Duck and Camp Lejeune, NC, Bay of Fundy, NS) despite spectral leakage problems in some of the image data (particularly severe in the Duck data). These spectral leakage problems increased the manual intervention or supervision for the waterline extraction process, but still produced reasonable results with data gaps. However, the vegetation line was easily extracted, at Duck, because the contrast was greater than at the waterline. A MHWL estimate was surveyed at Duck by NOAA and this was compared with the Duck extracted shorelines. *In situ* GPS measurements of the waterlines were compared with the image extracted waterlines for the other sites.

A shoreline extraction logic was based on associating image phenomenology with beach environment type. Consequently, for the extraction process, the selection of a waterline was based on image interpretation and oceanography and sedimentology beach models. This type of procedure is required since there are many beach types with different physical characteristics and corresponding different image phenomenology. For the sites studied here the logic was based on the ocean wave energy levels deduced from features in the imagery. This strategy resulted in reasonable shorelines for all the data studied here. For instance, Duck and Camp Lejeune which are separated by a distance of 300 km, have the same type of image phenomenology. The same logic for extracting a waterline was applied to both sites and resulted in waterline estimates with average errors consistent with the estimated experimental uncertainty. The Bay of Fundy's waterline estimates were based on a different phenomenology (i.e. less energetic waves), and logic for the waterline extraction. These extracted estimates were near the ground truthed waterline with average (maximum) errors of 7 m (30 m). The waterline signature dependency in the imagery on the physical environment emphasizes the requirement of conducting more case studies (which include ground truthing) for different types of environments not studied here. In particular, the arctic and mangrove swamp regions are two types of areas which should be studied. Also, areas with significant topographic change should be studied.
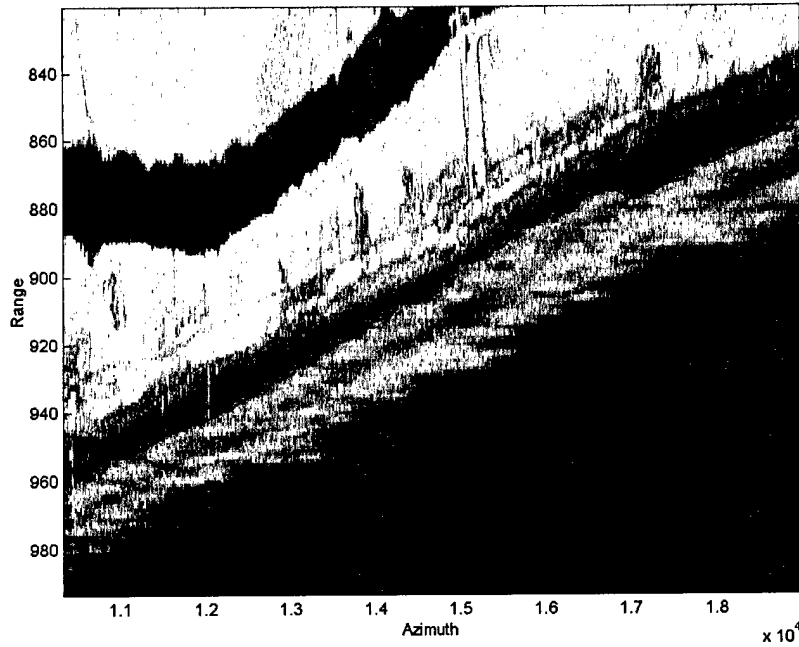
Figure 18. Camp Lejeune image in the background with an overlay in red of the extracted shoreline. Axes are in image coordinates. The image represents distances of about 900 m x 3600 m in range and azimuth dimensions.
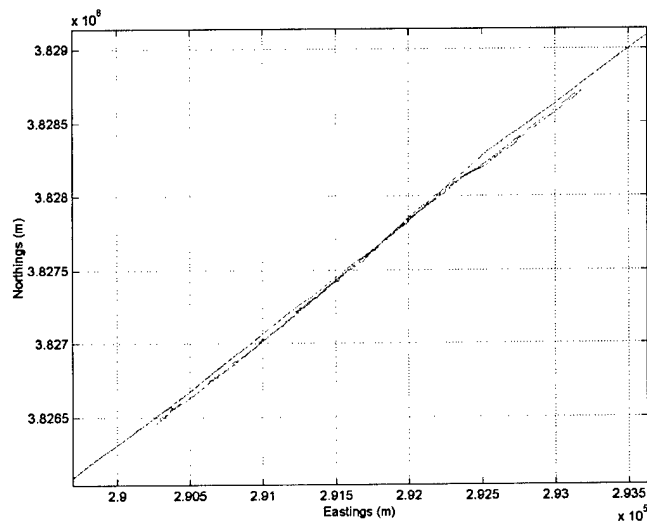
Figure 19. Comparison between the *in situ* GPS measurements (green), Lidar measurements (red) and the extracted shoreline (blue). Axes in Northings and Eastings coordinates.

Shoreline slopes were also studied at both Duck and Fundy. The shoreline slope estimates were not successful at Duck. It is not known if this is because of the spectral leakage problems, or because the beach was too narrow or too rough, or that the SAR (C-band) wavelength was not appropriate for these applications. The responses, used for this analysis, indicated several scatterer components instead of results that resemble a flat surface model. Since, the data quality improved over the nearby ocean, it suggests that this analysis was not suitable for this wavelength and shore surface combination. In contrast, low tide Bay of Fundy tidal flat data produced the expected shore slope results from responses which were qualitatively like empirical models of topographically flat surfaces. These results require further validation with ground truthed data.

Only one shoreline slope extraction method was studied in this report. This method and other shoreline slope extraction methods require further investigation with well ground truthed results from data such as LIDAR which measures topography and bathymetry.

A NIMA-DREO report [10] will discuss and compare all Duck extracted shoreline results with the surveyed MHWL. A comparison method specified by NIMA will be tested on shorelines extracted from Landsat, RADARSAT, LIDAR and other single and polarimetric SAR data. Initial comparisons indicated Landsat errors were about 30 m while supervised RADARSAT errors were about 6.5 m. Multi-temporal RADARSAT shoreline results had errors ranging from 7 to 25 m. One of the polarimetric results for the worst case (i.e. mean high tide comparison with low tide shoreline) had an error estimate of 6.3 m (using NIMA's error method). An alternative method, implemented in this report, had an error estimate of 6.8 m as shown in Table 2.

Perhaps the most significant point from this study is the importance of ground truthed comparisons. If ground truthing was not conducted for the North Carolina coastline, the wrong interpretations would have been made, resulting in less accurate shoreline estimates with average errors of about 30 m instead of 7 m.

These studies are with an airborne SAR which will have similar characteristics to Radarsat 2. However, the resolution will be coarser and the power from Radarasat 2 will be less, which will likely have an effect on Radarsat 2 results for some of the methods employed here.

4.3   Recommendations

On the basis of this study we make the following recommendations.

1. Conduct case studies (which include ground truthing) for any new regions if the environment is qualitatively different from previously studied areas, before proceeding with a complete shoreline extraction analysis. Particular areas which should be studied include: the arctic, mangrove swamps and regions with significant topographic changes.
2. Survey tidal elevations relative to the tidal statistics [8, 9]. In particular, surveying a reference tidal network (with good elevation accuracy) along a shoreline could be a consideration of the Global Shoreline project. As global tidal models improve and as the world is mapped more precisely, this information will complement other data bases for environmental modelling and mapping.

3. Acquire, if possible, *in situ* tidal elevations during the image acquisition for each region of analysis. [It is possible that satellites such as Topex-Poseiden or other satellites with altimeters could be used for this procedure and this requires further investigation.] Alternatively, tidal models can be used for predicting these elevations. However these predictions are not accurate because of daily variations due to storm cells and other environmental events.

4. Reference all the shorelines in geodetic coordinates (i.e. WGS 84). This will reduce the extra computation associated with transforming all the data into the same coordinate system particularly since all commercial satellite data and GPS data are referenced in these coordinates.

5. Further work should be devoted to sorting shoreline segments, orienting them in the correct direction and interpolating between them correctly. This was one problem we had with the analysis. In particular for the regions where the extracted shorelines had several data gaps. It was difficult and time consuming to connect all these segments together. Algorithms should be developed to do this automatically. See 8 below.

6. Classification methods (e.g. Cloude's coherency matrix methods) could be used for masking out areas outside the region of interest in order to reduce computational time.

7. Research other topographic / bathymetric slope extraction methods. These applications complement many other projects other than the Global Shoreline Project. Current studies [31, 32, 33] for extracting the bathymetry from images are making progress and look promising.

8. For extracted shorelines with many data gaps, determining a polynomial from the waterline vector segments may be a better method for describing the waterline in a region. In this way, when higher orders are removed, a better waterline estimate can be extracted, without the small scale temporal variations (i.e. wave undulations).

9. If the dual polarization mode is used (for RADARSAT 2), the most optimal channels indicated from this study are: HH for incidence angles > 45°, and the HV channel for detecting motion.

10. More effort is required to determine if data such as Topex-Poseiden data can be used to determine *in situ* ocean surface height data while the SAR data is imaged.

4.4 Further R&D

One of the important results learned from this study is the importance of ground truthing for verifying the interpretations and assessing different types of phenomenology. In particular, because of the different image phenomenology, the shoreline extraction method for the Bay of Fundy was not the same as that used for the North Carolina shoreline. This illustrates that different environments should be ground truthed and studied separately. The logic which pertains to one shoreline environment does not necessarily pertain to all.

One area which requires further investigation is the arctic area. RADARSAT images were acquired and studied but there were no conclusive results. This is a particularly difficult environment to interpret and can only be accomplished with well ground truthed experiments.

Other environments which need further investigation are: mangrove swamps, rainforests, coral reefs and mountainous regions. For this project, no regions with substantial cliffs were studied. This should be addressed in another study which incorporates InSAR or stereo methods.

5. Conclusion and perspectives

We have investigated polarimetric methods for extracting shorelines from SAR imagery. Two types of polarimetric applications were studied. One application was to extract the shoreline slope using polarimetric methods, in order to relate waterline measurements with tidal datum values. Since these slope values relate to the plane perpendicular to the SAR Line of Sight (LOS) only, this method would only be useful for imagery where the SAR path was perpendicular to the shoreline (such as the northern shoreline of Canada for the Radarsat satellites) or if Digital Elevation Maps (DEMs) were available. The other application studied is polarimetric methods which enhance the shoreline's land-water boundary. In addition, a shoreline extraction process was developed here so that from any analysed image (magnitude only) a shoreline can be extracted.

Image data from two regions were investigated for the polarimetric study of this project: Bay of Fundy, NS and North Carolina coastal sites (Duck and Camp Lejeune). *In situ* ground truthing and MHWL measurements were used to compare the extracted shorelines.

Methods which were employed for enhancing the contrast included the span, Pre-Whitening Filter (PWF), optimal polarization response filters, correlation / coherence between the HV and VH channels and coherence matrix classification methods which are based on the Wishart distribution. The phase difference between the two channels, HV and VH, was used as an indicator for regions where motion or target changes occurred. This phase difference was used as an exponential weight since it would bias positively (negatively) stationary (non-stationary) regions. Single channel data were also compared in order to assess whether polarimetric data was necessary for this project, particularly since the optimal polarization response for the Bay of Fundy was very near the HH component.

For regions like the Bay of Fundy, the extracted shoreline from a single channel, the HH component produced results which were near the experimental error. This was likely because the dynamic range between land and water was large for this area where the waves were relatively gentle.

In contrast the North Carolina waves are larger and more dynamic so that extracting shorelines from its imagery requires consideration of the shoreline phenomenology. The log(PWF) and log(cross-polarization coherence) produced reasonable shoreline vector results. An exponential weighting function using the phase difference between the HV and VH channels improved the shoreline estimates. The polarimetric discriminators generally produced better results than single channel data.

The Duck, NC data had significant spectral leakage in the imagery, associated with the SAR system, and, the land-water definition was less distinct than the Fundy data, which resulted in more manual supervision for extracting the waterline. Other influences, like SAR wave motion distortions (e.g. wave bunching), probably contributed to these less distinct shoreline regions where large waves occur. Camp Lejeune did not have the same spectral leakage problems and the shoreline extraction was relatively less comlex.

Reasonable waterline estimates were extracted for all of the shorelines studied here with average errors within 10 m and maximum errors about 30 m relative to a reference shoreline. These results are sufficient for many mapping requirements. For applications requiring a tidal reference (such as MHWL), the error between a waterline and MHWL is dependent on knowledge of the *in situ* tidal elevation (i.e. at the image time), local tidal constituents (i.e. tidal statistics) and the shore slope. Unfortunately, current global tidal data bases are not reliable or well maintained. Yet, high quality tidal information would contribute to many applications such as: mapping, navigation, storm assessment, global warming analysis, arctic open water predictions, meteorology / oceanographic predictions, environmental monitoring, disaster management and prediction (flooding and tsunamis). With a project like the Global Shoreline, some of these tidal variables should seriously be considered for present and future plans. This would facilitate the integration of tidal models into the analysis as they improve or become available and provide the ability to implement this information for many applications (as listed above) in the future. Acquiring *in situ* tidal elevations should be considered a part of this project.

Shoreline slope extraction was unsuccessful at Duck. It is not known whether the reason is because of saturation problems from land into the water or whether the beach region is too rough for the C-band data. The latter is considered more likely since the data quality over the nearby ocean was much better. Since the low tide Scots Bay, Fundy imagery was not available, a nearby region was studied instead. The quality of these shore slope results were significantly better than at Duck and the slope results were near the expected values. These results are promising but require further research since no ground truthing is presently available for this Fundy region.

Ocean sedimentology generalizations are often made about the wave action and beach particle sizes. Similarly, generalizations about the beach dynamics 'visible' from the imagery may be used for interpretation so that the correct shoreline is extracted. For the shorelines studied here, phenomenological differences such as the shore dynamics require consideration for extracting the required shoreline. This was not initially obvious for the imagery studied here, and indicates that any new environments require a case study where both ground truthing and imagery are acquired simultaneously.

In conclusion, from the three sites studied, waterline estimates, with average errors near the experimental error, have been extracted. There is the potential to improve these estimates to MHWL estimates if tidal and shore slope information are included into the analysis. Further work is required with well ground truthed data to study various shore slope extraction methods. For the Fundy, Nova Scotia coastline, which generally is a region with mild wave action, single channel data was adequate for extracting waterlines, although other methods produced slightly better results. In contrast, for more dynamical beach types, (e.g. North Carolina) the polarimetric discriminators and exponential weights (HV-VH phase difference) were required to extract the waterline. Beach slope extraction, from these images, produced some promising results, but requires further ground truthed studies. Classification methods such as coherence matrix methods using the Wishart distribution also provide shorelines and assist the interpretation and extraction process.

Further research for other environments is required since these results are based on only two environment types and the phenomenological interpretation for these two was different. In

particular, arctic and mangrove swamps are two types of shoreline that require further attention. Cliff type shoreline regions should be studied separately using other methods such as InSAR.

6. References

1. Beaudoin, A., Bucheit, M., Yeremy, M.. Global shoreline mapping from spaceborne SAR: Assessment for RADARSAT. Internal DREO report in progress.

2. Koopmans, B.N. and Wang, Y. (1995). ERSWAD project, Measurement of land-sea transition from ERS-1 SAR at different phases of tidal water. Final Report (ERS-1 verification project Coastal Zones NL8)', ISBN 90 5411, 1-64.

3. Mason, D., Davenport, I., Flather, R., McCartney, B. and Robinson, G. (1995). Construction of an Inter-Tidal Digital Elevation Model by the Waterline Method. *Geoph. Res. Letters*, vol 22, no 23, 3187—3190.

4. Mason, D. and Davenport, I.J. (1996). Accurate and Efficient Determination of the Shoreline in ERS-1 SAR Images. *IEEE Trans. on Geosc. And Rem. Sens.*, vol 34, no 5, 1243—1253.

5. Mason, D.C, Davenport, I.J., Flather, R.A., and Gurney, C. (1998). A Digital Elevation Model of the Inter-Tidal Areas of the Wash, England, produced by the Waterline Method. *Int. Jr. Rem. Sens.*, vol . 19, no 8, 1455—1460.

6. Thomson, A.G., Fuller, R.M. and Eastwood, J.A. (1998). Supervised versus Unsupervised Methods for Classification of Coasts and River Corridors from Airborne Sensing. *Int. Jr. Rem. Sens.*, vol 19, no. 17, 3423—3431.

7. Cracknell, A.P. (1999). Remote sensing techniques in Estuaries and Coastal Zones –an update. *Int., Jr. Rem. Sens.*, vol 19, no 3, 485—496.

8. O'Reilly, C.T., Parsons, S. and Langelier, D. (1996). A Universal Seamless Vertical Reference Surface for Hydrographical Bathymetry with Specific Applications to Seismic Areas. *Proc. Of the Int. Assoc. of Geod. Symposia*, Vol. 117, Tokyo, Japan, 736—743.

9. Parsons, S.A., O'Reilly, C.T. (1996). The Application of GPS Derived Ellipsoid Heights to Hydrographic Data Acquisitions and the Definition of Tidal Datums. *Proc. of the Canadian Hydrographical Conference '96*, Halifax, NS, 26—33.

10. NIMA–DREO Final Global Shoreline Report. In progress.

11. Boerner, W.-M., Mott, H., Luneberg, E., Livingstone, C., Briscoe, B., Brown, R.,J., Paterson, J.,S.. (1998). Polarimetry in radar remote sensing: basic and applied concepts. Ch. 5 In *Principles and Applications of Imaging Radar*. Eds. Henderson, F.M., and Lewis, A.J.. John Wiley and Sons, pp. 271-356.

12. Mott, H., (1992). *Antennas for Radar and Communications, A Polarimetric Approach*. John Wiley and Sons. pp. 521.

13. Huynen, J.R., (1987). Phenomenological Theory of Radar Targets. Ph.D. Thesis, P.Q. Research, Polarimetric Quest, Los Altos Hills, Ca., USA, pp 216.

14. Cameron, W.L., Youssef, N.N. and Leung, L.K., (1996). Simulated polarimetric signatures of primitive geometric shapes. *IEEE Trans. Geosc. and Rem. Sens.*, Vol 34, No 5, May 1996, pp. 793-803.

15. Cameron, W.L. and Leung, L.K., (1992). Identification of elemental scatter responses in high-resolution ISAR and SAR signature measurements. *Secondes Journees Internationales de la Polarimetrie Radar, IRESTE, Nantes, France*, Sept 8-10, 1992, pp 196-212.

16. Yeremy, M.L., Campbell, J.W.M., Mattar, K. and Potter, T., Ocean surveillance with polarimtric SAR. A DREO perspective on the future. submitted to the *Can. Jr. of Rem. Sens.*

17. Cloude, S.R. and Pottier,E. (1997). An Entropy Based Classification Scheme for Land Classifications of Polarimetric SAR. *IEEE Trans. Geosc. and Rem. Sens.*, Vol 35, 68—78.

18. Pottier, E. and Lee, J.S. (2000). Unsupervised Classification Scheme of POLSAR Images based on the Complex Wishart Distribution and the <<H/A/α>> Polarimetric Decomposition Theorem. *EURSAR2000, Munich, Germany*, May, 2000, pp. 265-268.

19. Lee, J.S., Grunes, M.R., Ainsworth, T.L., Du, L.J, Schuler, D.L. and Cloude, S.R. (1999). Unsupervised Classification Using Polarimetric Decomposition and the Complex Wishart Classifier. *IEEE Trans. Geosc . & Rem. Sens.*, Vol 37, No 5., 2249—2257.

20. Yeremy, M.L., Beaudoin, J.D., Walter, G.M. and Beaudoin, A. (2000). Shoreline mapping from SAR imagery: a polarimetric approach. *Proc. Of the 22nd Can. Rem. Sens. Symposium*, 21-25 Aug 2000, Victoria, BC. pp 10.

21. Fitch, J.P., The single antenna interferometer (1991). *IEEE Conference on Acoustics, Speed, and Signals*, Toronto, ON, 2573- 2576.

22. Tsang, L., Kong, J.A., Shin, R.T. (1985). Theory of Microwave Remote Sensing. John Wiley and Sons.

23. Galvin, C.J. (1972). Waves breaking in shallow water. In Meyer,R.D, (Ed), *Waves on Beaches and resulting sediment transport*, Academic Press, NY.

24. Thomson, R.E. (1983). Oceanography of the British Columbia Coast, Canadian Special Publication of Fish. And Aquatic Sc., No. 56.

25. Komar, P.P. (1976). Beach processes and sedimentation. Prentice Hall, NJ.

26. Livingstone, C.E., Gray, A.L., Hawkins, R.K., Vachon, P., Lukowski, T.I., and Lalonde, M. (1995). The CCRS Airborne SAR Systems: Radar for Remote Sensing Research. *Canadian Jr. of Rem. Sens.*, vol 21, no 4, pp 468—491.

27. Hawkins, R., K., Touzi, R., Livingstone, C.E., (1999). Calibration and use of CV-580 airborne polarimetric SAR data. *Proc. 4th International Airborne Rem. Sens. Conference and Exhibition, 21st Can. Symp. Rem. Sens.,* Vol 2, II.32-II.40.

28. Hawkins, R.,K., Vachon, P.W., (1998). C/X SAR gain and point target measurements – The saturation problem. CCRS Technical Note: CCRS-TN-1998-27. pp. 10.

29. Ed. Allan, T.D. (1983). Satellite Microwave Remote Sensing. Ellis Horwood Ltd.

30. Hennings, I. And Lurin, B. (2000). Radar Imaging of the Sea Bed during the C-Star Experiment in 1996: On the Determination of the Relaxation Rate Parameter of Short Gravity Waves due to Current Variations from In Situ Measurements and Theory. *IGARSS 2000,* Munich, Germany.

31. Vogelsang, J. (2000). Radar Imaging of Sea Bottom Topography under Various Azimuth Angles. *IGARSS 2000,* Munich, Germany.

32. Stolte, S. and Stolte, S. (2000). In-Situ Measurements of Short Wave Modulation due to Bottom Topography. *IGARSS 2000,* Munich, Germany.

33. Schuler, D.L., Lee, J.S., and De Grandi, G. (1996). Measurement of Topography Using Polarimetric SAR Images. *IEEE TGARS,* Vol 34, No 5, 1266-1277.

34. Lee, J-S, Schuler, D.L. and Ainsworth, T.L. (1999). Polarimetric SAR Data Compensations for Terrain Azimuth Slope Variations. submitter to *IEEE TGARS.*

35. Pottier, E. (1998). Unsupervised Classification Scheme and Topography Derivation of POLSAR Data on the <<H/A/α>> Polarimetric Decomposition Theorem. *Proc. Of the Fourth Int. Workshop on Radar Polarimetry', Nantes, France,* 538-548.

36. Novak, L.M., Burl, M.C. and Irving, W.W. (1993). Optimal Polarimetric Processing for Enhanced Target Detection. *IEEE Trans. Aerosp. & Electronic Systems,* Vol 29, No 1, 234—243.

37. Eds. Ulaby, F.T. and Elachi, C. (1990). Radar Polarimetry for Geoscience Applications. Artech House.

38. Zebker, H.A., van Zyl, J.J., Held, D.N. (1987). Imaging Radar Polarimetry from Wave Synthesis. *J.G.R.,* Vol. 92, No. B1, 683-701.

39. Swartz, A.A., Yueh, H.A., Kong, J.A., Novak, L.M. and Shin, R.T. (1988). Optimal Polarizations for Achieving Maximimum Contrast in Radar Images. *J.G.R.,* Vol. 93, No. B12, 15252—15260.

40. Lim, J.S. (1990). Two-Dimensional Signal and Image Processing. Englewood Cliffs, NJ, Prentice Hall,

41. Lee, J.S, Grunes, M.R. and de Grandi, G. (1999). Polarimetric SAR Speckle Filtering and its Implication for Classification. *IEEE Trans. Geosc. & Rem. Sens.*, Vol 37, No 5, 2363—2373.

42. Hawkins, R.K., CCRS, personal communication, 2000.

43. Walter, G., Yeremy, M. L., A Comparison of polarimetric classification methods. DREO report in progress.

List of symbols/abbreviations/acronyms/initialisms

ARC	Active Radar Calibrator
DEM	Digital Elevation Map
DND	Department of National Defence
DREO	Defence Research Establishment Ottawa
FRF	Field Research Facility
GCP	Ground Control Point
GPS	Global Positioning Systems
LIDAR	Light Detection and Ranging
MHWL	Mean High Water Line
MLWL	Mean Low Water Line
NIMA	National Imagery Mapping Agency
NOAA	National Oceanic and Atmospheric Administration
PRF	Pulse Repetition Frequency
PWF	Pre-Whitening Filter
SRTM	Shuttle Radar Topography Mapper

DOCUMENT CONTROL DATA

(Security classification of title, body of abstract and indexing annotation must be entered when the overall document is classified)

1. ORIGINATOR (the name and address of the organization preparing the document. Organizations for whom the document was prepared, e.g. Establishment sponsoring a contractor's report, or tasking agency, are entered in section 8.) Defence Research Establishment Ottawa	2. SECURITY CLASSIFICATION (overall security classification of the document, including special warning terms if applicable) UNCLASSIFIED

3. TITLE (the complete document title as indicated on the title page. Its classification should be indicated by the appropriate abbreviation (S,C or U) in parentheses after the title.)

Global shoreline mapping from an air-borne polarimetric SAR : Assessment for RADARSAT 2 polarimetric modes (U)

4. AUTHORS (Last name, first name, middle initial)

Yeremy, Maureen L., Beaudoin, Andre', Beaudoin, Jonathan D., and Walter, Gillian M.

5. DATE OF PUBLICATION (month and year of publication of document) November 2001	6a. NO. OF PAGES (total containing information. Include Annexes, Appendices, etc.) 60	6b. NO. OF REFS (total cited in document) 43

7. DESCRIPTIVE NOTES (the category of the document, e.g. technical report, technical note or memorandum. If appropriate, enter the type of report, e.g. interim, progress, summary, annual or final. Give the inclusive dates when a specific reporting period is covered.)

DREO Technical Report

8. SPONSORING ACTIVITY (the name of the department project office or laboratory sponsoring the research and development. Include the address.)

Defence Research Establishment Ottawa, 3701 Carling Avenue, Ottawa, ON, K1A 0Z4

9a. PROJECT OR GRANT NO. (if appropriate, the applicable research and development project or grant number under which the document was written. Please specify whether project or grant) 5eb14	9b. CONTRACT NO. (if appropriate, the applicable number under which the document was written)
10a. ORIGINATOR'S DOCUMENT NUMBER (the official document number by which the document is identified by the originating activity. This number must be unique to this document.) DREO Technical Report 2001-056	10b. OTHER DOCUMENT NOS. (Any other numbers which may be assigned this document either by the originator or by the sponsor)

11. DOCUMENT AVAILABILITY (any limitations on further dissemination of the document, other than those imposed by security classification)

(x) Unlimited distribution
( ) Distribution limited to defence departments and defence contractors; further distribution only as approved
( ) Distribution limited to defence departments and Canadian defence contractors; further distribution only as approved
( ) Distribution limited to government departments and agencies; further distribution only as approved
( ) Distribution limited to defence departments; further distribution only as approved
( ) Other (please specify):

12. DOCUMENT ANNOUNCEMENT (any limitation to the bibliographic announcement of this document. This will normally correspond to the Document Availability (11). However, where further distribution (beyond the audience specified in 11) is possible, a wider announcement audience may be selected.)

DCD03 2/06/87

13. ABSTRACT (a brief and factual summary of the document. It may also appear elsewhere in the body of the document itself. It is highly desirable that the abstract of classified documents be unclassified. Each paragraph of the abstract shall begin with an indication of the security classification of the information in the paragraph (unless the document itself is unclassified) represented as (S), (C), or (U). It is not necessary to include here abstracts in both official languages unless the text is bilingual).

A project between two agencies, DREO and NIMA was initiated in 1998 to study shoreline extraction from imagery. DREO researched SAR applications with an emphasis on Radarsat products. The focus of this report is the extraction of shorelines from polarimetric SAR imagery in preparation for the launch of Radarsat 2.The desired vector shoreline product for this project is the Mean High Water Line (MHWL). This specification implies that consideration of tidal models are required. For this project in addition to radar considerations, geomatics, topographic and oceanographic issues were considered part of the investigation. Polarimetric classification methods were used to detect the shoreline region. Contrast enhancement methods were implemented to emphasize the shoreline edge. The cross-polarized channels provided velocity information which was used for discriminating between non-stationary (i.e.; ocean) and stationary surfaces (i.e.; land). One method for extracting shore slopes was studied here to determine if it is feasible for C-band SAR data. Two experimental trials acquired polarimetric SAR image data for each study site at both the high and low tide extremes. In situ ground truthing was conducted while the image data was collected. The trial locations were at Fundy, NS, and the North Carolina (NC) coast. Comparisons were made with either GPS vector data collected at the waterline during the acquisition time, or a surveyed MHWL vector estimate. Phenomenological differences between the shore types were observed and are documented here. One method to extract shore slopes was studied and did not produce reasonable results for the North Carolina site and reasonable results for the NS site. Further work is required here. A mean error estimate between a waterline extracted from an image, acquired at low tide, and a surveyed MHWL was 6.3 m over a 2 km vector. The error of uncertainty is about 7.0 m. In general, all image waterline estimates when compared to the in situ ground truthed waterlines had average errors of about 7 m and maximum errors of about 30 m.

14. KEYWORDS, DESCRIPTORS or IDENTIFIERS (technically meaningful terms or short phrases that characterize a document and could be helpful in cataloguing the document. They should be selected so that no security classification is required. Identifiers such as equipment model designation, trade name, military project code name, geographic location may also be included. If possible keywords should be selected from a published thesaurus. e.g. Thesaurus of Engineering and Scientific Terms (TEST) and that thesaurus-identified. If it is not possible to select indexing terms which are Unclassified, the classification of each should be indicated as with the title.)

shoreline vector extraction, global shoreline project, image extraction, image detection, image classification, polarimetric SAR image data, C-band SAR, Radarsat, Radarsat 2
polarimetric methods: span, coherence, correlation, Wishart Distribution, decomposition methods (Cameron, Huynen, Cloude, Pottier, Lee), topographic slope extraction, polarimetric filters

Defence R&D Canada

is the national authority for providing

Science and Technology (S&T) leadership

in the advancement and maintenance

of Canada's defence capabilities.

R et D pour la défense Canada

est responsable, au niveau national, pour

les sciences et la technologie (S et T)

au service de l'avancement et du maintien des

capacités de défense du Canada.

DEFENCE DÉFENSE

www.drdc-rddc.dnd.ca